Université Mohamed Khider de Biskra
Faculté des Science Exactes et de des Sciences de la nature et la vie
Département des Sciences de la matière

MÉMOIRE DE MASTER

Domaine Sciences de la Matière
Filière de chimie
Chimie des matériaux
Réf. : CH19

Présenté et soutenu par :
Hachemi Fadoua Aridj

Le : 12/06/2024

Effect of doping and sintering temperature on the structural properties of a dielectric ceramic

---

Jury :

Mr	**Mahmoud OMARI**	**Prof**	**Université de Biskra**	**Président**
Mr	**Abdelhek MEKLID**	**MCA**	**Université de Biskra**	**Rapporteur**
Mme	**Zelikha NECIRA**	**MCA**	**Université de Biskra**	**Examinatrice**

Année universitaire : 2023/2024

Acknowledgements

*First of all, I would like to thank **Allah**, the Almighty, for giving me the strength, courage, patience and willpower to carry out this modest work.*

All of this work took place at the Chemistry Laboratory of the Department of Matter Sciences at the University of Biskra.

*I would particularly like to thank **Mr. Abdelhek Meklid**, who supervised and provided me with guidance throughout the period during which I was writing this thesis. I would like to express my gratitude to him for having passed on to me his sense of pedagogy and his attention to detail.*

*I would also like to express my respectful thanks to the members of the jury: **Mr. Mahmoud Omari** and **Mrs. Zelikha Necira** for the honor they have done us by agreeing to judge this work.*

I would also like to thank all the Chemistry Laboratory Engineers in our Department for the for the material help and means they made available to us, to carry out this research work.

*I would like to mention **Mrs. Hayet Benmachiche**, Head of Laboratory, **Mrs. Nadia Bouzize**, **Mrs. Soumia Khelifa**, who provided me with the Infrared Spectrometry analyses.*

I also owe a debt of gratitude to all the chemistry teachers who followed me during my studies, and all of those who contributed in any way to the success of this work.

Finally, I would like to warmly thank my friends and colleagues who have always helped and encouraged me.

My sincere thanks.

Fadoua Aridj Hachemi.

Dedication

To my mother and father, for

The education they lavished on me with all the means and at the price of all the sacrifices they made for me, for the sense of duty they taught me since my childhood.

To my dear brothers: Dhia Eddine, Ahmed

To my dear sisters: Tesnim, Amina, Chahd Layen

To the soul of my grandfathers and my uncle

To all my friends and colleagues whom I have known since childhood

To all the teachers who have taught me throughout my career

To all those who love me, To all those whom I love

I dedicate this modest work to you.

Abstract

The main objective of this work focuses on the synthesis and structural and physical characterization of a new PZT-type ceramic material with an ABO_3 perovskite structure. More specifically, the study focuses on the ternary system:

$Pb_{1-y}Ca_y[Zr_xTi_{0.98-x}(Fe_{1/5}Zn_{1/5}Sb_{3/5})_{0.02}]O_3$, abbreviated as **PCZT-FZS**, with **x = 0.49, 0.50** and **y = 0.05**.

Substitution at the A and B sites was carried out to improve its physical properties.

The samples chosen for this study were prepared using a solid-state synthesis method, and at different sintering temperatures: 1100°C, 1150°C, 1200°C and 1250°C respectively in order to optimize the optimum sintering temperature where the density of the samples is maximum (close to the theoretical density) and therefore the product is of better physical quality.

Various techniques were used to characterize our samples, including X-ray diffraction (XRD), scanning electron microscopy (SEM) and IR analysis.

The results indicate that sample no.1 (49/49) has a tetragonal structure with a density of 77.74%.

Key words: perovskite, PZT, dielectric, tetragonal.

Résumé

L'objectif principal de ce travail se concentre sur la synthèse et la caractérisation structurale et physique d'un nouveau matériau en céramique de type PZT et de structure pérovskite ABO_3. Plus précisément, l'étude porte sur le système ternaire :

$Pb_{1-y}Ca_y[Zr_xTi_{0,98-x}(Fe_{1/5}Zn_{1/5}Sb_{3/5})_{0,02}]O_3$, abrégé en **PCZT-FZS**, avec **x = 0.49, 0.50** et **y = 0.05**.

Une substitution en sites A et B a été effectuée pour améliorer ses propriétés physiques.

Les échantillons choisis pour cette étude ont été préparés à l'aide d'une méthode de synthèse à l'état solide, et à différentes températures de frittage :1100°C, 1150°C, 1200°C et 1250°C respectivement afin d'optimiser la température de frittage où la densité des échantillons est maximale (près de la densité théorique) et donc le produit est de meilleur qualité physique.

Diverses techniques ont été utilisées pour caractériser les échantillons telles que la diffraction des rayons X (DRX), la microscopie électronique à balayage (MEB) et l'analyse IR.

Les résultats indiquent que l'échantillon n°1 (49/49) a une structure tétragonale avec une densité de 77,74%.

Mots clés : pérovskite, PZT, diélectrique, tétragonale.

ملخص

الهدف الرئيسي من هذا العمل هو اصطناع وتحديد الخصائص البنيوية والفيزيائية لمادة جديدة من السيراميك من نوع PZT ذات بنية البيروفسكيت ABO_3 وبشكل أكثر تحديدًا، تركز الدراسة على النظام الثلاثي:

$Pb_{1-y}Ca_y[Zr_xTi_{0,98-x}(Fe_{1/5}Zn_{1/5}Sb_{3/5})_{0,02}]O_3$ ، ويرمز له اختصارًا بـ : **PCZT-FZS**، مع : **x = 0.49, 0.50** و **y = 0.05**.

تمت دراستنا بإجراء استبدال في الموقعين A وB من أجل تحسين هذه الخصائص الفيزيائية.

تم تحضير العينات المختارة لهذه الدراسة باستخدام الطريقة الكلاسيكية (في الحالة الصلبة)، وفي درجات حرارة تلبيد مختلفة: 1100°م، 1150°م، 1200°م و1250°م على التوالي من أجل تحديد درجة حرارة التلبيد المثلى حيث تكون كثافة العينات عالية (قريبة من الكثافة النظرية) وبالتالي يكون المنتج ذو خصائص فيزيائية أفضل .

استُخدمت تقنيات مختلفة لتحديد خصائص العينات، بما في ذلك حيود الأشعة السينية (DRX)، والمجهر الإلكتروني الماسح (MEB) وتحليل الأشعة تحت الحمراء (IR).

تشير النتائج إلى أن العينة رقم 1 (49/49) لها بنية رباعية الزوايا بكثافة 77.74%.

الكلمات المفتاحية: بيروفسكيت، PZT، عازل كهربائي، رباعي الزوايا.

Contents

Contents

Contents

General Conclusion

Figures List

Chapter I : General Information and Definitions

Figures List

Chapter II : Experimental Techniques

Figures List

Chapter III : Structural and morphological study of the PCZT-FZS solid solution

Figures List

Tables List

Chapter I : General Information and Definitions

Chapter II : Experimental Techniques

Chapter III : Structural and morphological study of the PCZT-FZS solid solution

General Introduction

General Introduction

Since piezoelectric ceramics were developed in the 20th century, their material properties have been widely studied by a large number of scientists around the world. Recently, one of the most popular piezoelectric ceramics is lead zirconate titanate (PZT), which has a perovskite structure **[1]**.

In this work we focus on PZT solid solutions. Lead zircono-titanates of the general formula Pb (Zr_x, Ti_{1-x})O_3 have been widely developed for their good dielectric, ferroelectric and piezoelectric properties.

Oxide-based compounds of the general formula Pb (Zr_x, Ti_{1-x})O_3 with a perovskite (ABO_3) structure, known as PZT, have particularly interesting properties. They are ferroelectric over a wide range of temperatures, including room temperature. In fact, they are materials that lend themselves well to experimental investigations and are used in the industrial manufacture of many electronic components such as high-frequency devices, resonators, electromechanical transducers, sensors, electrical capacitors, piezoelectric motors, etc **[2]**.

Piezoelectric ceramics Pb (Zr_x, Ti_{1-x})O_3 attest to the importance of these materials in the vicinity of the morphotropic phase boundary where the two phases coexist and exhibit the highest values of dielectric constant and coupling factor. This boundary separates the two ferroelectric phases, one tetragonal and the other rhombohedral **[3]**.

The characteristics of these materials depend on their microstructure, which in turn is entirely determined by the chemical composition and the production process. These characteristics are generally improved by the addition of one or more cations which will replace the Pb^{+2} in site (A) and/or the couple (Zr^{+4}/Ti^{+4}) in site (B) of the perovskite. The right choice of additive raw materials and the optimization of certain conditions for forming PZT powders, in particular the calcination process, are therefore essential **[4,5]**.

Our objective is therefore to develop, synthesis and characterize a new substituted ceramic material with the general formula: $Pb_{0.95}Ca_{0.05}[Zr_xTi_{0.98-x}(Fe_{1/5}Zn_{1/5}Sb_{3/5})_{0.02}]O_3$, hereafter abbreviated to PCZT-FZS.

This thesis is organized as follows:

In Chapter 1 we simplify the basic concepts of piezoelectric ceramics, the perovskite lattice structure and PZT solid solutions.

The second chapter presents the experimental method used to prepare our PCZT-FZS sample, as well as the physicochemical, morphological and structural characterization techniques.

In the last one, we interpret the results of the structural characterization of $Pb_{0.95}Ca_{0.05}[Zr_xTi_{0.98-x}(Fe_{1/5}Zn_{1/5}Sb_{3/5})_{0.02}]O_3$ as a function of sintering temperature and zircon concentration using several experimental techniques.

Finally, we close this thesis with a general conclusion, summarizing and discussing all the results obtained.

Bibliographic References

[1] M.Okayasu, Smart Energy Materials of PZT Ceramics, International Journal on Smart Material and Mechatronics, Vol.2, 2015, pp. 102-105.

[2] R.K.Abdelli, Synthèse et caractérisation d'un matériau de la structure pérovskites à base plomb, Mémoire de Master, Université Mohamed Khider-Biskra- Algérie ,2018.

[3] F.Kahoul, L.Hamzioui, A.Boutarfaia, Synthèse et caractérisation de nouvelles céramiques PZT-SFN. International Days of Organometallic Chemistry and Catalysis JICOC Ouargla, 2012, pp. 58-67.

[4] A.Meklid **,** Elaboration, caractérisation et étude des propriétés diélectriques et électromécaniques d'un nouveau matériau de céramique de type Zirconate-Titanate de plomb (PZT)**,** Thèse de doctorat, Université Mohamed Khider-Biskra-Algérie,2018.

[5] N. Abdessalem, A. Boutarfaia, M. Abba, Z. Necira, The Effect of Addition of Nd^{3+} on Dielectric Properties of Pb $[Zr_{0.45}Ti_{0.45}(Zn_{1/3}, Sb_{2/3})_{0.1}]O_3$ System, Journal of Fundamental and Applied Sciences, Vol.3, 2011, pp. 126-132.

Chapter I

General Information and Definitions

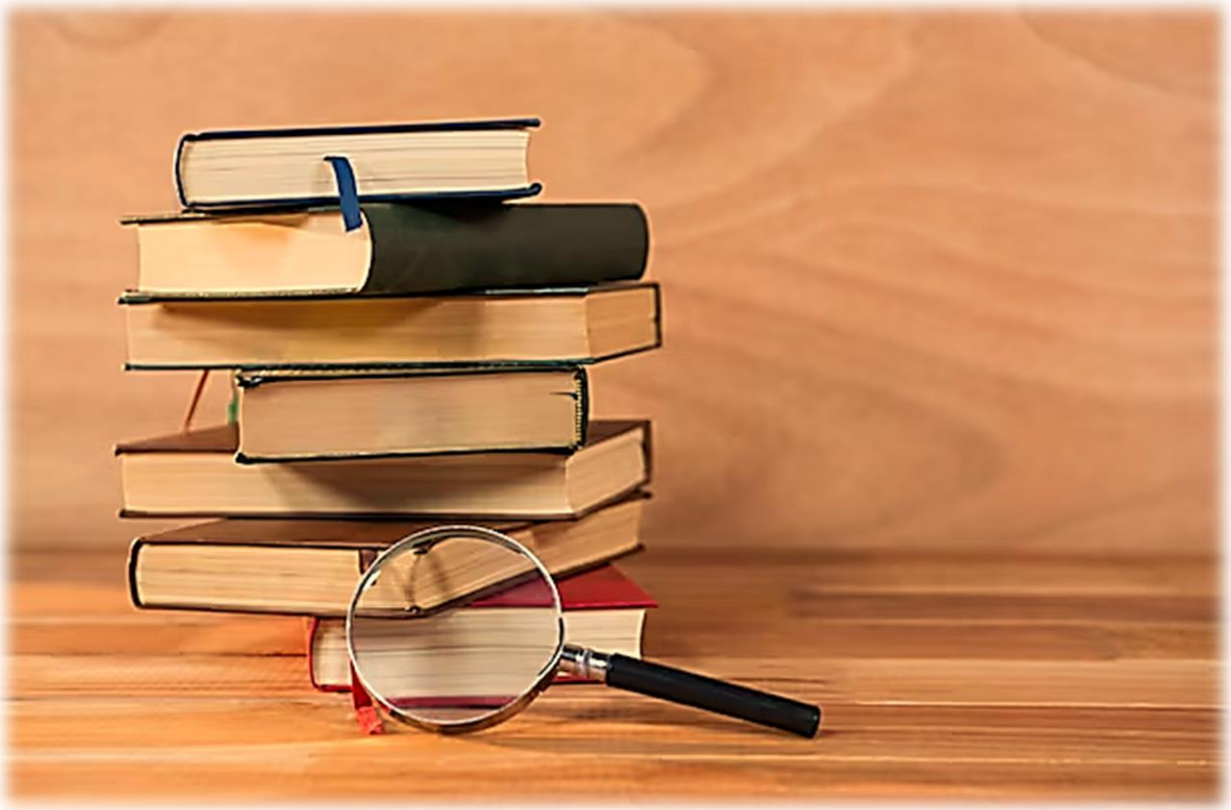

I.1. Introduction

Ceramics are solid synthetic materials that often require thermal treatments in order to be produced. Most modern ceramics are prepared from consolidated powders (shaping) and are densified by thermal treatment, the process of densification is known as sintering. There are two categories of ceramics: traditional ceramics (like those found in pottery), and technical ceramics.

Technical ceramics with the general formula $Pb(Zr_xTi_{1-x})O_3$ (PZT), are inorganic and non-metallic materials obtained by shaping a powder and subjecting it to high-temperature thermal treatment. They are known for its exceptional durability and rigidity (support very high tensions). They are resistant to heat, wear, chemical agents, and corrosion. However, they can be quite fragile and prone to breakage under heavy stress, despite this; Lead zirconate-titanate (PZT) ceramics are widely used in the electronics industry for their excellent piezoelectric properties and low cost. They are used in electrical capacitors, headphones, microphones, high frequency devices and in the field of wireless telegraphy **[1]**.

I.2. Ceramic materials

I.2.1. Definition

The word ‘ceramics’ comes from the Greek word ‘keramos’, which means ‘clay’. This term is often used to describe traditional items such as pottery, porcelain and bricks, but more generally it means a solid that is neither a metal nor a polymer.

Ceramics are produced by sintering a mixture of oxides. The manufacturing process can be modified to adjust their composition, which in turn can affect their dielectric, mechanical, and piezoelectric performances **[2-4]**.

I.2.2. General properties of ceramics

It could be argued that ceramic materials possess diverse properties. In The table below presents a number of general properties of ceramic materials.

Table I.1: Different properties of ceramics

Chemical properties	• Resistant to ageing and climatic or chemical aggression. • High chemical inertness. • Resistant to corrosion.
Physical properties	• Excellent electrical insulators. • Resistant to thermal shock. • Low thermal conductivity. • Refractory. • Very high melting temperature.
Mechanical properties	• High mechanical strength. • No ductility or toughness. • High hardness. • Fragile. • High resistance to wear.

These general properties derive from the nature of their chemical bonds, crystalline and microstructure **[3]**.

I.2.2.1. Chemical bonds

A distinction is made between ceramics that are predominantly covalent and those that are predominantly ionic in their atomic bonds. We therefore have a combination of two ionic and covalent bonds, known as iono-covalent bonds (**Fig.I.1**). The general properties resulting from these bonds are as follows:

- Ion-covalent ceramics have a filled valence band and a completely empty conduction band. This explains the poor conductivity of electricity and heat by ceramics. They are therefore used as dielectrics and thermal insulators.
- Ionic and covalent bonds are particularly stable and strong, which makes the melting temperatures of ceramics very high. They are therefore widely used as refractory materials **[2,3].**

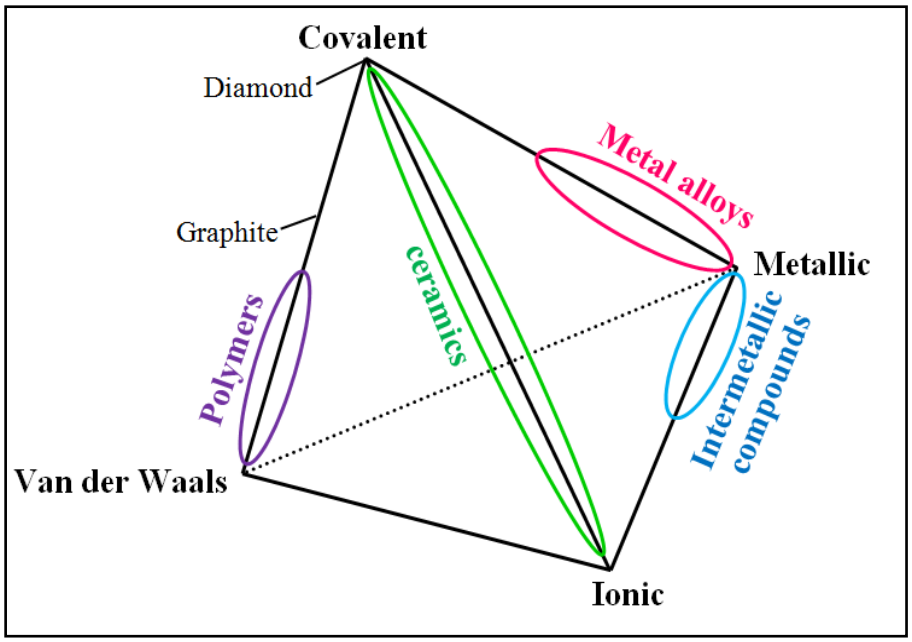

Figure I.1: Lustration of the different types of bonds, as well as the bonding area for ceramics and glass [2].

I.2.2.2. The microstructure

Crystalline ceramics form polycrystalline microstructures with a complex structure of grains and grain boundaries (**Fig.I.2**). Each grain is a more or less perfect single crystal.

The structure of the grain boundaries is more complex because the electrostatic interactions between the ions bring additional equilibrium constraints (ions of the same sign must always avoid each other). As a result, a fraction of porosity is frequently found in ceramics **[1]**.

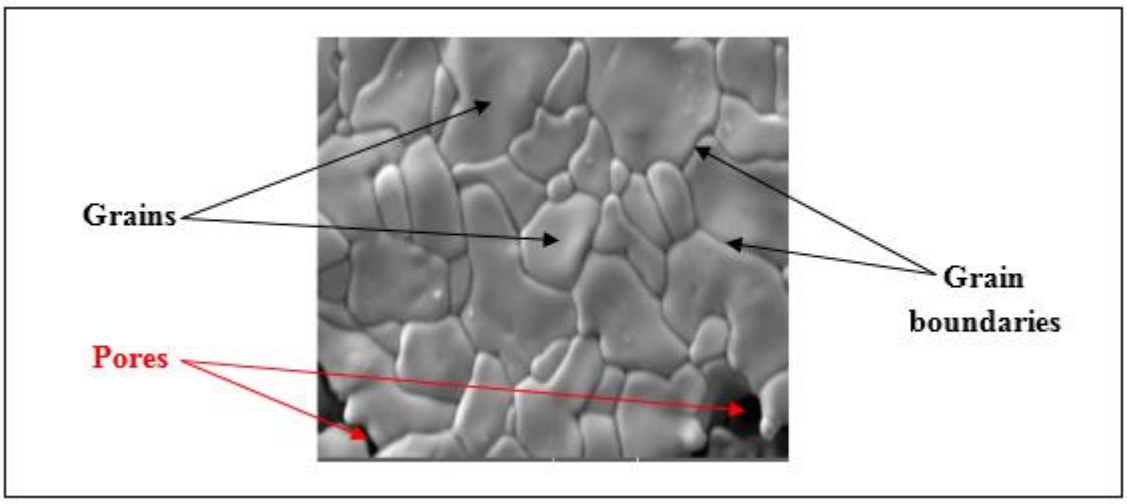

Figure I.2: Typical microstructure of a polished ceramic surface [2].

I.2.3. Physical properties of ceramics

I.2.3.1. Piezoelectricity

Etymologically, the prefix "piezo" comes from the Greek and means to squeeze or press. Piezoelectricity can be defined as a coupling phenomenon between elastic (mechanical) energy and electrical energy, manifested at the scale of the crystal lattice. These piezoelectric effects can only be observed on insulators **[1,2,5]**.

There are two types of piezoelectric phenomena:

- **Direct piezoelectric effect:** This is the power of a material to transform mechanical energy into electrical energy (a mechanical action causes the appearance of an electrical dipole in each mesh of the material by displacement of the centers of the positive and negative charges (**Fig.I.3**)) **[1,6]**.
- **Converse (Inverse) piezoelectric effect:** This is the power to transform electrical energy into mechanical deformation (the application of an external electric field induces mechanical deformation of the material **(Fig.I.3)**).

It was the Curie brothers who observed and explained the direct effect in 1880. But it was Lippmann who theoretically suggested the opposite effect, which was confirmed experimentally by the Curie brothers **[1,3, 6,7]**.

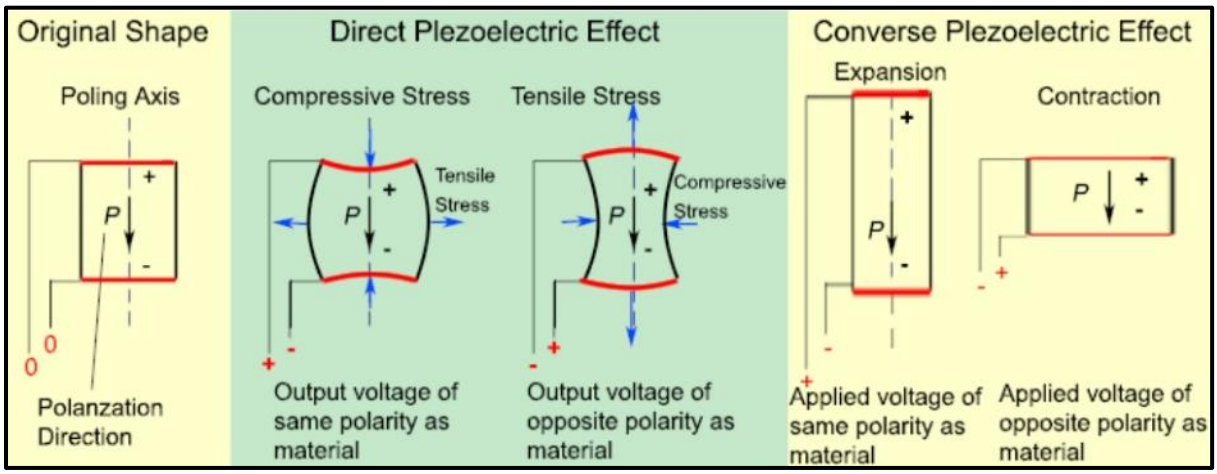

Figure I.3: Direct and inverse piezoelectric effects [8].

I.2.3.1.1. Piezoelectricity and symmetry

In crystalline solids, piezoelectricity is directly linked to the symmetry of the crystals and manifests itself as a polarization of the lattice. This dipole moment is created by separation of the center of gravity of the positive and negative charges as a result of deformation under stress.

The symmetry properties of crystals are of fundamental importance for the existence or non-existence of piezoelectricity. Any crystals with a center of symmetry cannot be piezoelectric, whereas crystals without a center of symmetry can be (**Fig.I.4**) **[3]**.

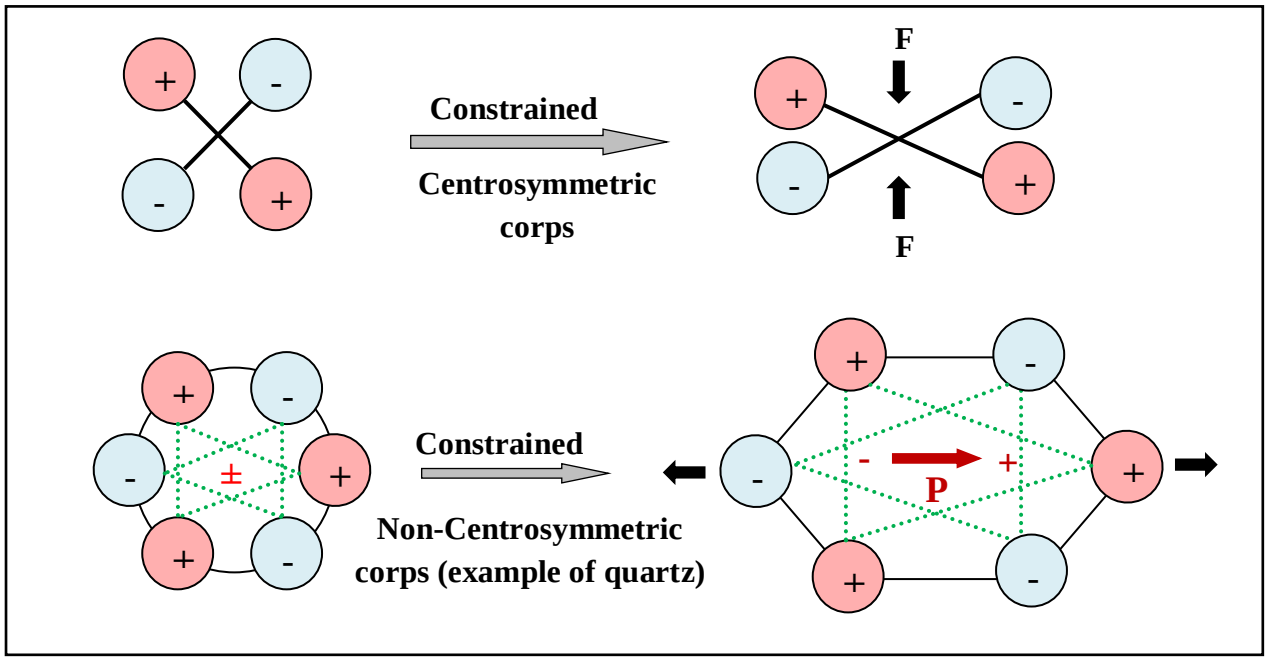

Figure I.4: Schematic appearance of piezoelectricity [9].

In crystallography, all structures are classified according to 32 classes of symmetry. 11 of these classes are said to be centrosymmetric and therefore cannot exhibit polar properties or spontaneous polarization. One of the other 21 classes has symmetry elements that prevent it from exhibiting polar characteristics (non-piezoelectric). The remaining 20 classes are piezoelectric, of which 10 are pyroelectric, i.e. they are electrically polarized in the absence of an applied electric field. They are called pyroelectric because of the variation in the amplitude of the dipole moment with temperature. Pyroelectric crystals include ferroelectric crystals in which the polar axis, the carrier of a permanent dipole, is mobile in the crystal lattice under the influence of an external electric field.

The breakdown of the 32 crystal classes according to these different names is summarized in (**Fig.I.5) [1]**.

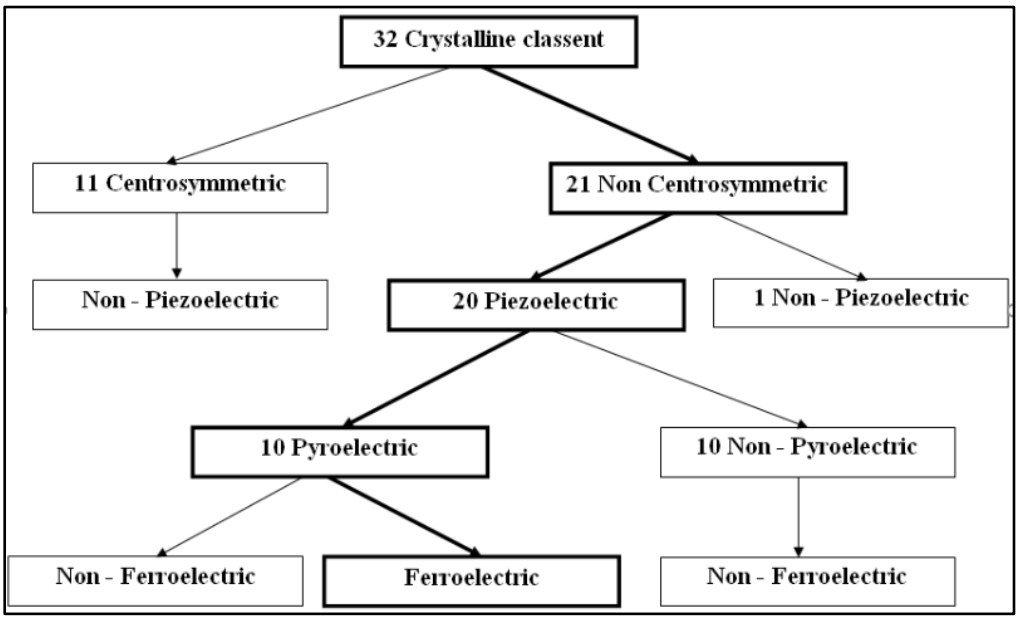

Figure I.5: Distribution of crystalline classes according to certain physical properties of materials [10].

I.2.3.2. Pyroelectricity

Pyroelectricity is a phenomenon that occurs when an insulating material undergoes a change in temperature, resulting in spontaneous polarization. This is caused by the relaxation of electrical charges due to thermal variation within the material. It is worth noting that pyroelectric materials belong to the subclass of piezoelectric materials. This class of materials is considered polar, as they exhibit spontaneous polarization even in the absence of an external electric field. It is worth noting that the degree of polarization is temperature-dependent **[8,11]**.

I.2.3.3. Ferroelectricity

Pyroelectric crystals exhibit spontaneous polarization within specific temperature ranges and can have their polarization reversed by an external electric field, resulting in them becoming ferroelectric crystals. Ferroelectric materials, which are a subcategory of pyroelectric materials, can polarize along multiple axes, allowing for permanent and mobile dipoles within the crystal structure when influenced by an external electric field.

Ferroelectricity is commonly defined as the intrinsic property of certain materials to exhibit spontaneous and permanent polarization without the need for an external electric field. It is worth noting that this polarization can be reversed by applying an electric field in the opposite direction. Ferroelectric materials can crystallize in different structures, including the perovskite structure, and exhibit a characteristic hysteresis cycle.

A ferroelectric crystal is typically composed of domains, which are homogeneous regions separated by domain walls. It is worth noting that each domain has a different polarization direction compared to its neighboring domains. The arrangement of these domains follows mechanical and electrical compatibility conditions, which can significantly affect the material's response to external electric fields.

The electrical properties of ferroelectric materials are determined by their structure and molecular composition. These materials can be produced as polycrystalline ceramics or single crystals **[1-3,5-7,9-13]**.

I.2.3.3.1. Ferroelectric domains

Ferroelectric crystals are composed of domains, which are regions with different polarization directions separated by domain walls. When no external field is present, the domains have random orientations, making the material non-polar. However, when an electric field is applied, the polarization directions of the domains undergo a reorientation process. This leads to an increase in the number of domains aligned with the applied field and/or the disappearance of domains with opposite polarization. In materials with a tetragonal and rhombohedral structure, domains at 180° completely flip over without changing the lattice structure. On the other hand, domains at 71° and 109° in rhombohedral structure, as well as 90° in tetragonal structure, induce significant lattice deformation, causing partial reorientation. The process of polarizing a ferroelectric ceramic is illustrated qualitatively in (**Fig.I.6**) **[1]**.

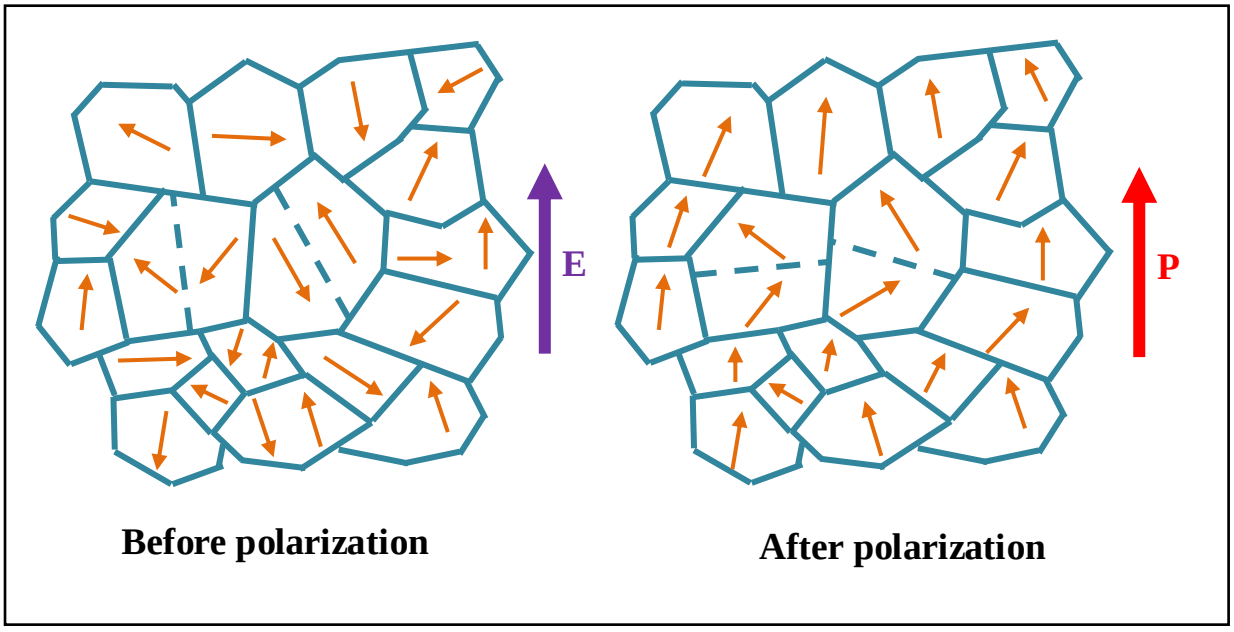

Figure I.6: Orientation of ferroelectric domains under the effect of an electric field [12].

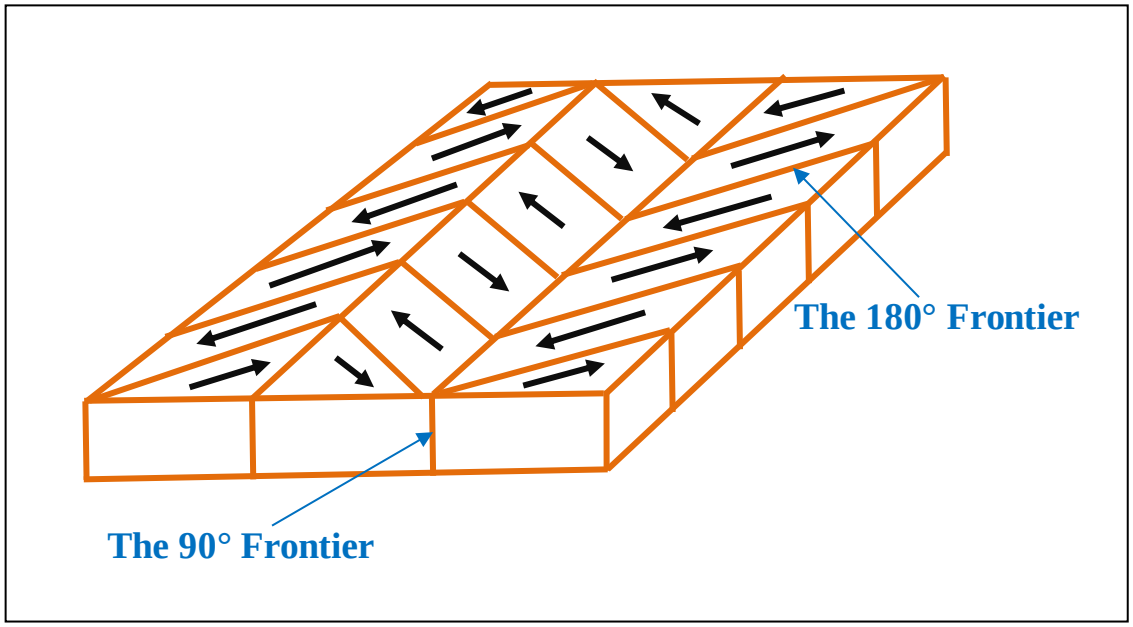

Figure I.7: Schematic illustration of 180° and 90° domain walls [12].

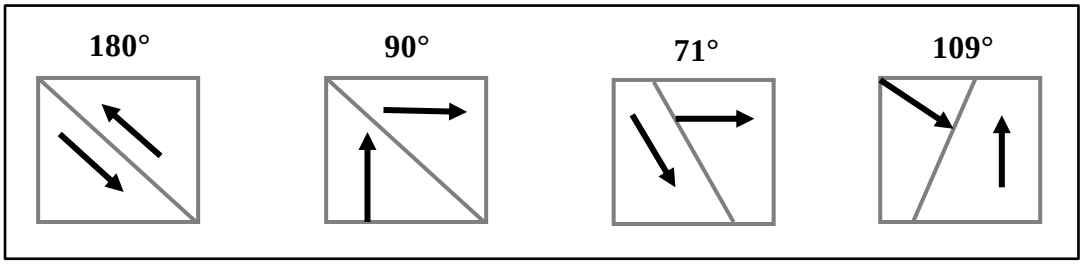

Figure I.8: Ferroelectric domains in a ceramic material [1].

I.2.3.3.2. The Curie point

The Curie point T_C is the temperature at which a ferroelectric material undergoes a structural phase transition to a state where spontaneous polarization disappears. At the Curie point, the relative dielectric permittivity ε_r ($\varepsilon_r = \varepsilon / \varepsilon_0$) reaches a maximum value. Above T_C, the ferroelectric material becomes paraelectric, which is reflected by a peak in the permittivity versus temperature curve.

The temperature and dielectric constant in many ferroelectric materials above the curie point are governed by the Curie-Weiss law:

$$\varepsilon = \varepsilon_0 + \frac{C}{(T - T_0)} \dots\dots\dots\dots\dots (I.1)$$

Where:

ε: is the dielectric permittivity of the material.

ε_0: the dielectric permittivity of vacuum.

C: is the curie constant.

T_0: is the Weiss curie temperature.

The Weiss curie temperature is often different from the **T_C** curie point (the temperature at which ε is maximum). For first-order transitions, **$T_0 < T_C$** whereas for second-order transitions, **$T_0 = T_C$ [12,14]**.

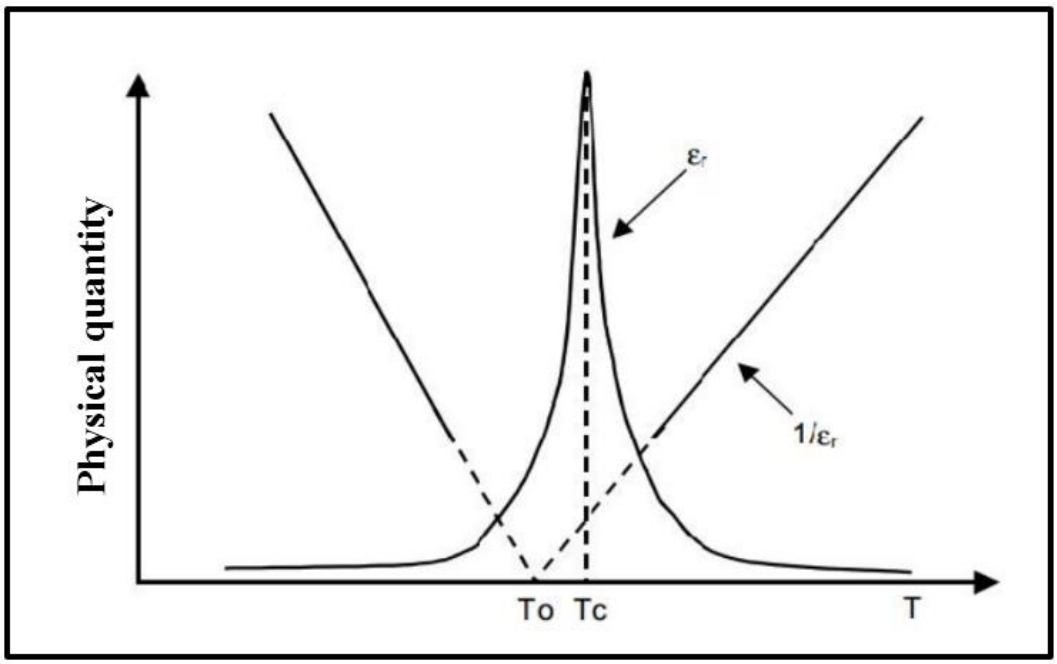

Figure I.9: Evolution of the dielectric permittivity of a ferroelectric as a function of temperature [1].

I.2.3.4. Dielectricity

A dielectric is a non-conductive medium made up of atoms or molecules that are electrically neutral. While they cannot conduct electric current, dielectric media can still exhibit certain electrical characteristics. When subjected to an external electric field, the charges within the dielectric are slightly displaced. Although the electrons cannot move over long distances, they can oscillate around the nucleus, creating electrostatic dipoles. Similarly, the overall movement of atoms within the material can also create dipoles. Dielectric materials polarize when placed in an electric field, forming elementary dipoles that align with the field. However,

unlike ferroelectrics, the polarization of a perfect dielectric is cancelled once the electric field is removed. Materials such as glass and plastics are examples of dielectric media **[2,5]**.

I.2.3.4.1. Polarization of a dielectric

The interesting property of a dielectric is that it polarizes under the action of an electric field. The dielectric then behaves like a set of elementary dipoles which orient themselves in the direction of the electric field (**Fig.I.10**). It should be noted that whatever the dielectric used, free charges remain which are the cause of dielectric losses **[12]**.

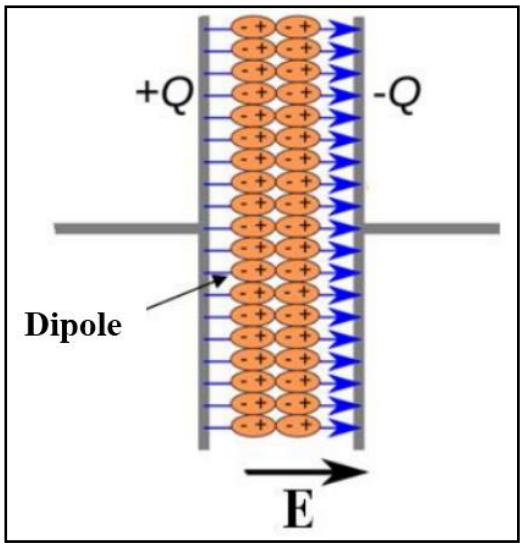

Figure I.10: Representation of the polarization of a dielectric material [1].

It is important to note that, in a dielectric, different types of polarization can occur for different frequencies (**Fig.I.11**) **[1].**

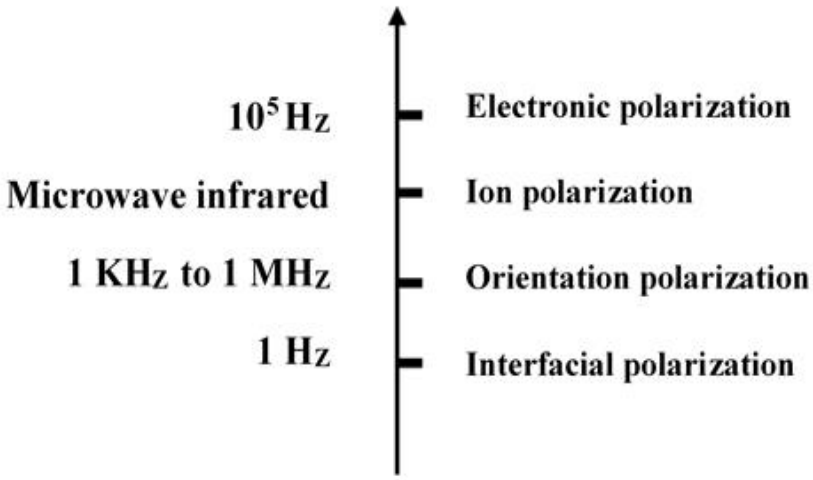

Figure I.11: Different types of polarization [12].

These types of polarization originate from different phenomena:

- Electronic polarization occurs when the center of mass of the nucleus and the electronic cloud of the atoms are no longer the same.
- Ionic polarization occurs when the center of mass of the Ba^{+2} and Ti^{+4} ions (in the case of $BaTiO_3$) is no longer that of the O^{-2} ions.
- Orientation polarization occurs when polar molecules in a medium seek to align their charge under the effect of an electric field. This phenomenon describes the behavior of electrochemical capacitors.
- Interfacial polarization is linked to the free movement of electronic charges within grains. These charges accumulate around defects in the structure, such as grain boundaries. Each grain of the material then becomes a dipole, with charges accumulating on its opposite walls.

The variation in polarization indicates that these phenomena are more or less effective as a function of polarization. This means that these phenomena are not perfect and are largely responsible for the losses in the material **[12]**.

I.2.3.4.2. Dielectric properties

I.2.3.4.2.1. Relative dielectric permittivity (ε_r) or dielectric constant

A material's dielectric constant (ε) or dielectric permittivity represents its ability to store charge. The higher the dielectric constant of a material, the greater its ability to store charges. When a dielectric material is inserted between the plates of a capacitor (**Fig.I.12**), its capacity becomes:

$$C = \frac{\varepsilon . S}{e} \quad \ldots\ldots\ldots\ldots\ldots (I.2)$$

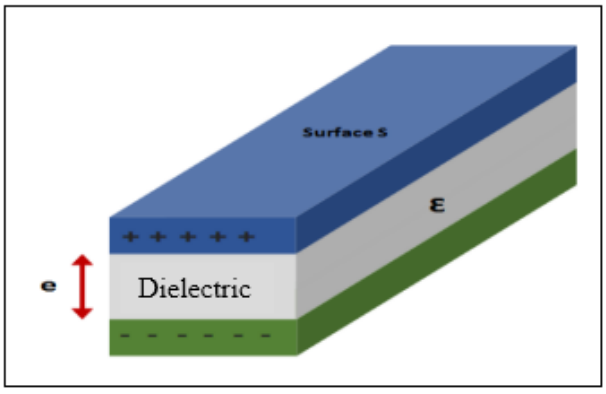

Figure I.12: Simplified diagram of a flat capacitor [9].

The relative dielectric permittivity (ε_r) of the dielectric medium is defined by:

$$\varepsilon_r = \frac{C}{C_0} \dots\dots\dots\dots\dots (I.3)$$

Depending on the frequency of the applied electric field, different types of polarization can be distinguished: an electronic contribution (≈10^{15} Hz), an ionic contribution (≈10^{13} Hz), a dipolar contribution (≤10^{8} Hz) and an interface contribution (<10^{3} Hz) **[9]**.

I.2.3.4.2.2. Dielectric losses

The dielectric loss factor is defined as the ratio between the energy dissipated and that supplied by the applied voltage. These losses reflect the delay or phase shift δ between the variation in the electric field and that of the induced polarization **[1]**.

I.2.3.4.2.3. Dielectric dissipation factor tg δ

If we apply an alternating electric field (AC voltage) to a perfect dielectric, the polarization changes charge (direction) with each alternation. The resulting current is a quarter of a period ahead of the voltage (ideal phase shift).

In the case of a real dielectric, the polarization changes direction with the field but with a certain delay. The electric current is therefore out of phase by an angle of δ compared with the ideal phase shift. This leads to energy dissipation, or dielectric losses.

The dielectric dissipation factor tg δ defines the deviation of the current-voltage phase shift from the ideal, as shown in **[15]**: $tg\delta = \frac{\varepsilon_{r_2}}{\varepsilon_{r_1}} \dots\dots\dots\dots\dots (I.4)$

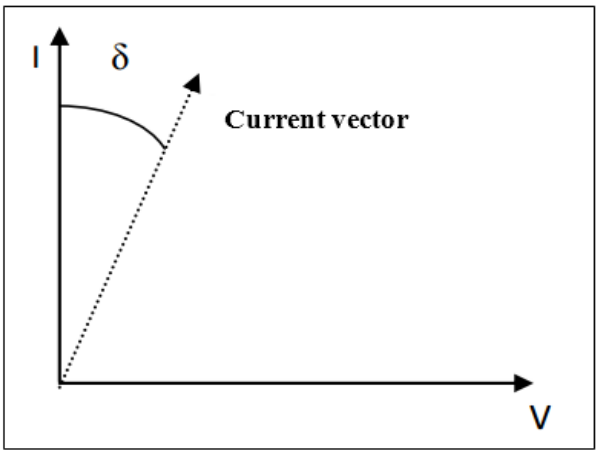

Figure I.13: Fresnel construction showing the current-voltage phase shift in the case of a capacitor and defining the angle of loss [15].

I.2.3.4.2.4. Dielectric strength

Any dielectric material subjected to an electric field permanently loses its insulating properties if the field exceeds a critical value, to which a breakdown voltage corresponds. The corresponding parameter is therefore the breakdown voltage gradient, called dielectric strength and expressed as a voltage per unit length.

Electrical stiffness is used to determine the minimum thickness of insulation to be used at a given voltage to avoid breakdown (sudden passage of current through the insulation); when the temperature rises, the breakdown voltage decreases.

Dielectric strength depends on many factors such as porosity, grain size and homogeneity **[5]**.

I.2.3.5. Ageing

The properties of ferroelectric materials subjected to repeated mechanical, electrical or thermal stresses can be modified and decrease significantly over time. This phenomenon, known as ageing, is linked to the progressive variation in the configuration of domain walls over time. The latter arrange themselves in a more stable configuration that minimizes the energy of the piezoelectric ceramic. In some materials, this gives rise to an internal field E_i in the opposite direction to the polarization axis, which significantly reduces the remnant polarization.

The variation in piezoelectric properties over time is generally expressed as follows **[12]**: $\mathbf{X(t) = X\,(t_0) + \ln \frac{t}{t_0}} \ldots\ldots\ldots\ldots\ldots (\mathbf{I.5})$ where:

$\mathbf{t_0}$: is the starting point of the measurement.

A: corresponds to the ageing rate.

X: represents the piezoelectric quantity under consideration.

I.2.3.6. Elasticity

Young's modulus (modulus of elasticity) expresses the rigidity of a material, i.e. the property of a material to deform in a reversible elastic manner under the action of a stress. Its formula is given by the relationship:

$$E = \frac{\text{Constraint}}{\text{Deformation}}\left(\frac{N}{m}\right) \ldots\ldots\ldots\ldots\ldots (I.6)$$

The size of the Young's modulus depends on the strength of the atomic bonds **[16]**.

I.3. Piezoelectric materials: lead zircono-titanates

The first piezoelectric materials based on lead zirconate titanate (PZT) were developed as early as 1954. The excellent piezoelectric properties of these ceramics were demonstrated by Jaffe, Roth and Manzullo. Today, PZTs are used in the manufacture of many ferroelectric transducers. In fact, they have replaced barium titanate ($BaTiO_3$) ceramics in many cases, because they perform better **[12]**.

I.3.1 Description of perovskite structure

The perovskite-type structure **ABO_3** crystallizes in its simplest form in a cubic lattice if A is taken as the origin of the lattice. In this structure, A is a divalent cation with a large radius and twelve co-ordination. Eight A cations form the cubic lattice. The oxygen ions are at the center of each face and form an octahedron at the center of which is the B cation, which must have a very small radius. It is tetravalent and has co-ordination six. (**Fig.I.14**) shows the cubic perovskite lattice with lead at the origin. In this system, the B ion is at the center of an octahedron of **BO_6** oxygens. The octahedra are linked together at the apices to form a three-dimensional network of BO_6 octahedra (**Fig.I.15**). As the octahedral site can be occupied by ions of different sizes, this leads to distortions in the perovskite lattice. It is these distortions that give the material its ferroelectric character, since the cubic lattice is paraelectric **[1]**.

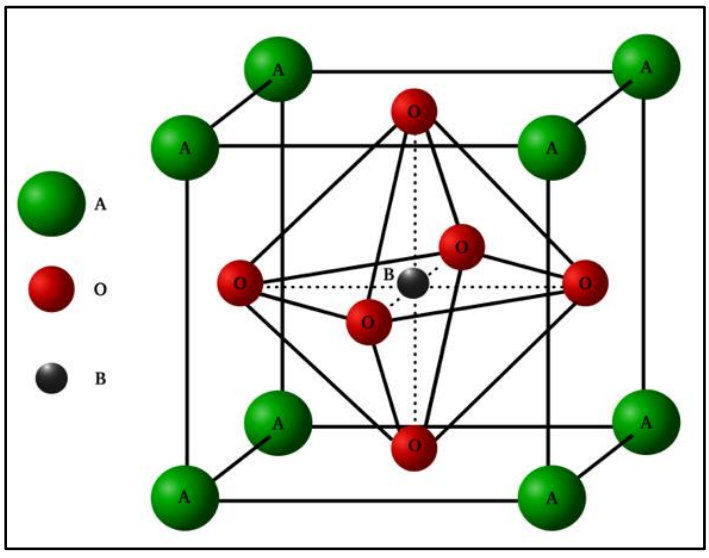

Figure I.14: Cubic perovskite lattice of PZT.

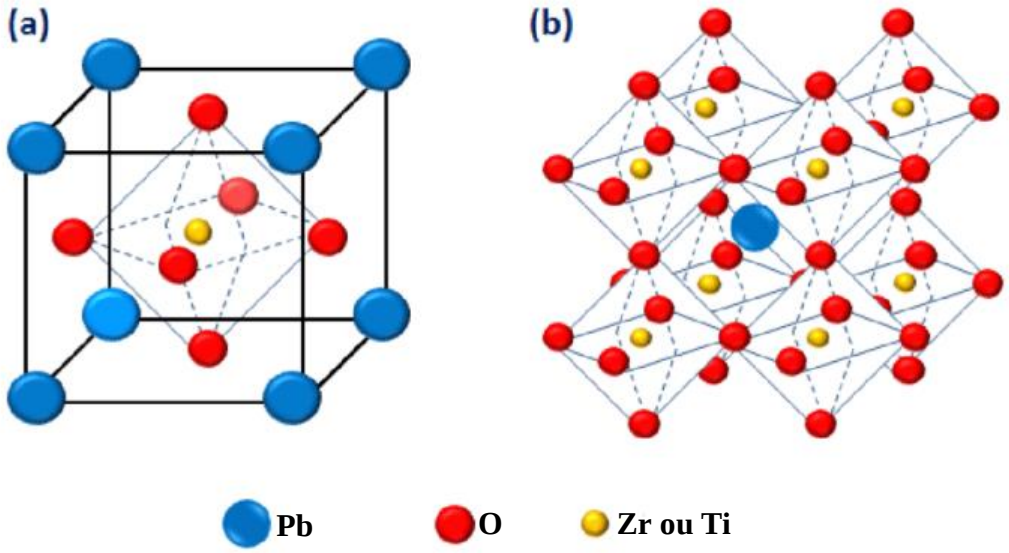

Figure I.15: Representation of the three-dimensional lattice of octahedral.

I.3.1.1. Simple perovskites

Simple perovskites, whose A and B sites are respectively occupied by a single type of atom: $BaTiO_3$, $KNbO_3$, $PbTiO_3$. . . etc **[3]**.

I.3.1.2. Complex perovskites

Complex perovskites, where one of the two sites A and B are occupied by two types of atoms: $Na_{0.5}Bi_{0.5}TiO_3$ (**BNT**), $PbMg_{1/3}Nb_{1/3}O_3$ (**PMN**), $K_{0.5}Bi_{0.5}TiO_3$ (**KBT**). The two sites A and B can also be substituted simultaneously: $(Pb_{1-x}Ca_x)$ (Zr_yTi_{1-y}) O_3 (**PCZT**) **[3]**.

I.3.1.3. Reception rates

The perovskite structure is characterized by a low hosting rate, so high interstitial concentrations are unlikely because the possible interstitial sites in the perovskite unit cell are bounded by positive and negative ions. The only site occupied is octahedral, in the center of the lattice, by a B^{4+} atom where it is surrounded by 6 O^{2-} anions. Each of the other three octahedra is formed by 4 O^{2-} anions and 2 A^{2+} cations and is unoccupied **[7]**.

I.3.2. Conditions for the structural stability of perovskite

Any solution with a perovskite structure must satisfy the following conditions:

I.3.2.1. Electroneutrality condition

Let be the following compound: $(\mathbf{A_1^1A_2^2A_3^3}\ldots\mathbf{A_n^K})(\mathbf{B_1^1B_2^2B_3^3}\ldots\mathbf{B_n^L})\mathbf{O_3}$

The cations A and B must satisfy:

$$\sum_{i=1}^{K} \mathbf{X_{A_i} n_{A_i}} + \sum_{j=1}^{L} \mathbf{X_{B_j} n_{B_j}} = +6 \ldots\ldots\ldots\ldots\ldots (\mathbf{I.7})$$

$\mathbf{X_{Ai}}$: being the molar fraction of cation A_i.

$\mathbf{X_{Bj}}$: being the mole fraction of cation B_j.

$\mathbf{n_{Ai}}$: valence number of cation A_i.

$\mathbf{n_{Bj}}$: valence number of cation B_j.

I.3.2.2. Stoichiometric condition

$$\sum_{i=1}^{K} \mathbf{X_{A_i}} = \mathbf{1}\ , \mathbf{0} \leq \mathbf{X_{A_i}} \leq \mathbf{1} \ldots\ldots\ldots\ldots\ldots (\mathbf{I.8})$$

$$\sum_{j=1}^{L} \mathbf{X_{B_j}} = \mathbf{1}\ \ , \mathbf{0} \leq \mathbf{X_{B_j}} \leq \mathbf{1} \ldots\ldots\ldots\ldots\ldots (\mathbf{I.9})$$

I.3.2.3. Geometric condition

The radius of the cations must obey the relationship:

$$\mathbf{t} = \frac{(\bar{\mathbf{R}}_{\mathbf{A_i}} + \mathbf{R_O})}{\sqrt{\mathbf{2}}(\bar{\mathbf{R}}_{\mathbf{B_j}} + \mathbf{R_O})} \ldots\ldots\ldots\ldots\ldots (\mathbf{I.10})$$

With:

$$\bar{\mathbf{R}}_{\mathbf{A_i}} = \sum_{i=1}^{K} \mathbf{X_{A_i} R_{A_i}} \ldots\ldots\ldots\ldots\ldots (\mathbf{I.11}) : \textbf{ Average radius of atoms } \mathbf{A_i}.$$

$$\bar{\mathbf{R}}_{\mathbf{B_j}} = \sum_{j=1}^{L} \mathbf{X_{B_j} R_{B_j}} \ldots\ldots\ldots\ldots\ldots (\mathbf{I.12}) : \textbf{ Average radius of atoms } \mathbf{B_j}.$$

It is advantageous for the A and B cations to be in contact with the O^{-2} anions to form a stable structure. The structure is therefore more stable the closer the factor **t** is to unity, and when **t > 1** the ferroelectric phase will be stable, whereas if **t < 1** the antiferroelectric phase will be the most stable. The radius of the B ion in the range **0.6 - 0.7 Å** seems to be a favorable condition for producing ferroelectricity **[2,12]**.

Table I.2: Evolution of crystal structures as a function of the value of the tolerance factor [2].

<table>
<tr><td rowspan="2">t < 0.75
Ilmenite</td><td colspan="3">0.75 < t < 1.06
Perovskite</td><td rowspan="2">t > 1.06
Hexagonal</td></tr>
<tr><td>0.75 < t < 0.96
Orthorhombic distortion</td><td>0.96 < t < 0.99
Rhombohedral distortion</td><td>0.99 < t < 1.06
Cubic</td></tr>
</table>

I.3.3. Classification of piezoelectric ceramics

I.3.3.1. Barium Titanate $BaTiO_3$

Barium Titanate is the most studied of the ferroelectric compounds. $BaTiO_3$ is a chemically and mechanically very stable compound that possesses ferroelectric properties over a temperature range that includes room temperature. $BaTiO_3$ belongs to the ABO_3 family of perovskites and has piezoelectric properties. It is widely used in capacitors because of its high dielectric constant (greater than 1000). It has a Curie temperature of 393°C and is prepared by heating at high temperature.

$$\mathbf{BaCO_{3\,(s)} + TiO_{3\,(s)} \rightarrow BaTiO_{3\,(s)} + CO_{2\,(g)}}$$

Its symmetry class at room temperature is 4mm **[7]**.

I.3.3.2. Lead Titanate $PbTiO_3$

Lead titanate is obtained by the reaction:

$$\mathbf{TiO_{2\,(s)} + PbO_{(s)} \xrightarrow{350-600°C} PbTiO_{3\,(s)}}$$

The reaction is accompanied by a slight release of heat. $PbTiO_3$ has a Curie temperature of 490°C and is ferroelectric like $BaTiO_3$. Above the Curie temperature it is paraelectric and has cubic symmetry with the lattice parameter: a = 3.96 Å at T = 535°C, whereas it is ferroelectric below the Curie temperature and has quadratic symmetry and the lattice parameters are: a = 3.894 Å, c = 4.14 Å and c/a = 1.132 **[7]**.

I.3.3.3. Lead zirconate $PbZrO_3$

Lead zirconate is obtained by the reaction:

$$\mathbf{ZrO_{2(s)} + PbO_{(s)} \xrightarrow{750-900°C} PbZrO_{3(s)}}$$

Lead zirconate undergoes an allotropic transformation at 230°C, which separates the stability domain of the antiferroelectric variety and the ferroelectric variety, so this temperature is defined as the Curie temperature. The antiferroelectric variety is orthorhombic, while the paraelectric variety is cubic. The lattice parameters of the orthorhombic variety are: a = 5.87 Å, b = 11.74 Å, c = 8.10 Å **[7]**.

I.3.3.4. Lead Zirconate Titanate PZT

Lead Zircono-Titanates (PZT) are prepared from a binary mixture of $PbTiO_3$ (ferroelectric) and $PbZrO_3$ (antiferroelectric). This mixture is miscible in all proportions. The piezoelectric and dielectric properties of the $Pb(Zr_{1-x}Ti_x)O_3$ solid solutions are much better than those of the initial compounds. The properties of these PZTs are optimal in the vicinity of the composition Zr/Ti = 0.48-0.52, which corresponds to the phase transition between two crystallographic systems **[7]**.

I.3.4. Phase diagram of solid solutions of $Pb(Zr_x,Ti_{1-x})O_3$

Above the Curie temperature, it is in the cubic phase that PZT crystallizes, below this temperature T, different structures become possible depending on the ratio of Zr and Ti. We can classify these structures according to the Zirconium content noted "x" in the generic formula: $Pb(Zr_xTi_{1-x})O_3$.

- For **x > 0.55**, we are in the zirconium-rich range and the crystallization phase has a rhombohedral structure. PZT has a permanent dipole moment.

- For **x < 0.45**, we are in the titanium-rich domain and this time the crystallization phase has a quadratic structure.

- For a value of **x between 0.45 and 0.55**, we have a mixture of the two structures, called the morphotropic phase boundary. In this range, the piezoelectric properties of PZT are at their best.

(**Fig.I.16**) shows the phase diagram of PZT as a function of the percentage of lead titanate in solid solution in lead zirconate, the two being miscible in any proportion. We can note that a small zone corresponding to a ceramic with a low titanium content is anti-ferroelectric (noted AF), the grey part is the morphotropic zone **[5]**.

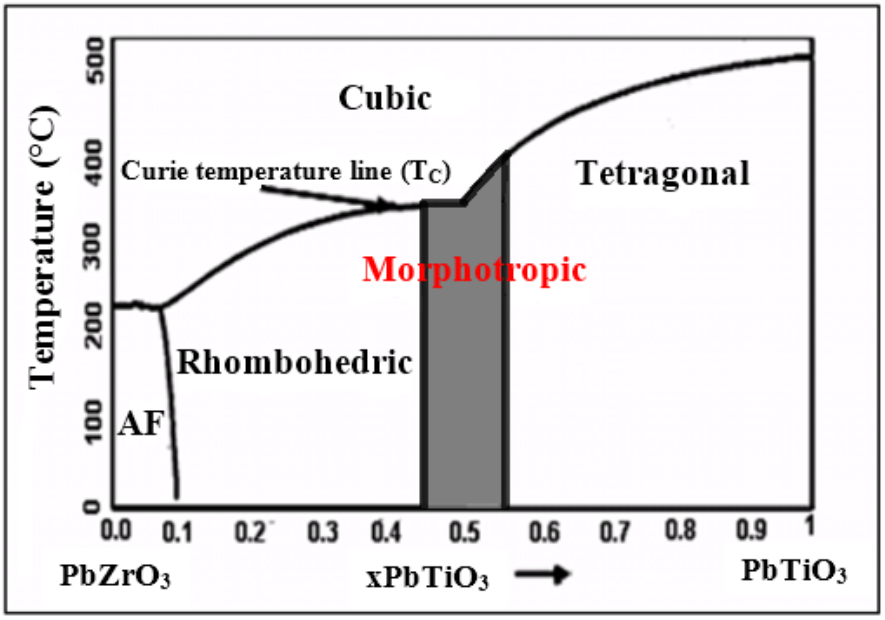

Figure I.16: Phase diagram of $Pb(Zr_xTi_{1-x})O_3$ taken from Jaffe et al (the grey area is the morphotropic zone) [5].

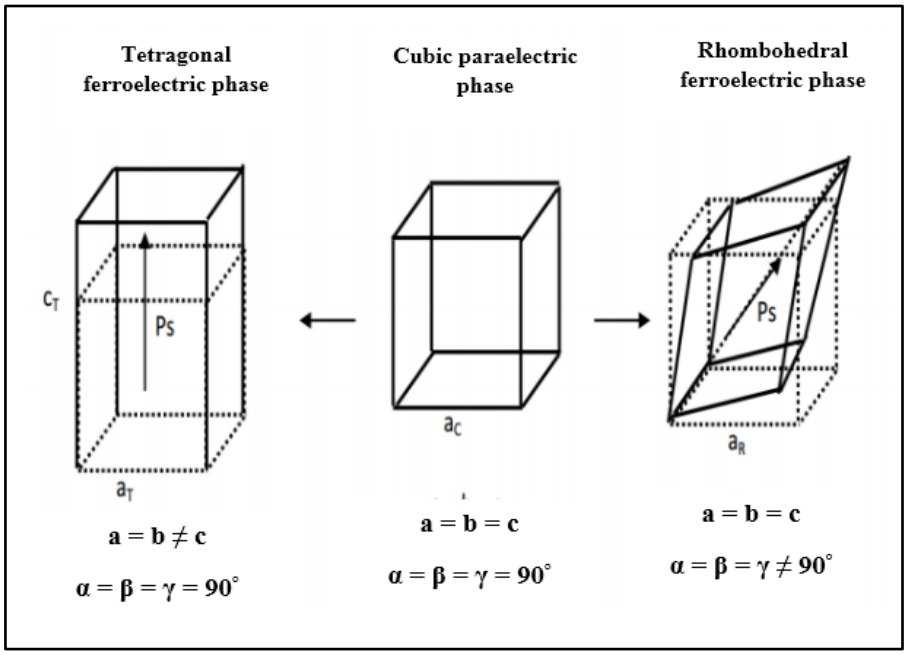

Figure I.17: Possible deformations of the PZT structure [2].

I.4. Effect of doping on piezoelectric properties

I.4.1 Doping of PZT

The remarkable properties (di-, piezo-, ferro-electric, etc.) of PZT ceramics in the morphotropic zone can be considerably modified by the substitution of one or more foreign cations which will replace the Pb^{2+} in the A-sites of the perovskite structure (ABO_3) or the couple (Zr^{4+}/Ti^{4+}) in the B-sites and sometimes anions to replace the oxygen, in which case the material is said to be doped. It should be noted that dopants call on different affinities linked mainly to the difference in size between two ions (ionic radius) or to their difference in electronegativity. (**Fig.I.18**) shows the chemical elements that can occupy sites A and B in the perovskite structure ABO_3 **[17].**

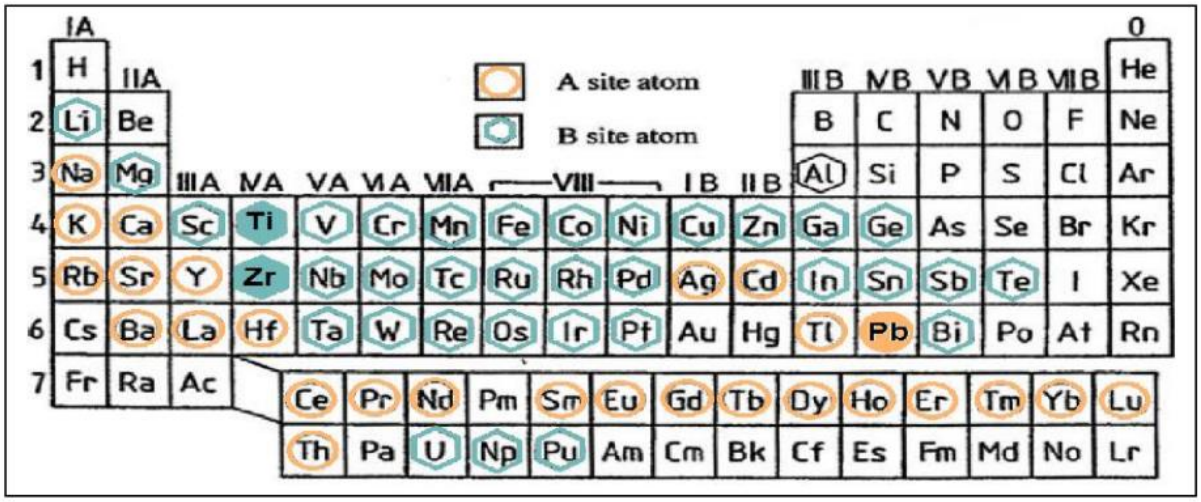

Figure I.18: Chemical elements that may occupy sites (A and B) in the ABO_3 perovskite structure [17].

The presence of doping elements leads to the appearance of distortions in the mesh. There are two main parameters that determine the stability of the perovskite structure after doping: The Goldschmidt factor and the ionicity of the bonds.

Dopants are generally classified into three categories according to their valency and that of the ion isovalent dopants, donor dopants and acceptor dopants **[17]**.

I.4.2. Classification of dopants

I.4.2.1. Substitution with an isovalent dopant (with a valency equal to that of the substituted ion)

The use of isovalent dopants such as Ba^{2+}, Sr^{2+}, Ca^{2+}at A sites and Ce^{4+}at B sites in perovskite has not been well developed in studies of PZT doping.

Nevertheless, it should be noted that these dopants increase the ionic character of the lattice, resulting in a decrease in the Curie point and an increase in the dielectric permittivity of PZT at room temperature **[16]**.

I.4.2.2. Substitution by an acceptor dopant whose valency is lower than that of the site it replaces

PZT materials doped with acceptors are said to be hard because they depolarize with difficulty under stress. Acceptor dopants behave differently from undoped PZTs, including: a rapid decrease in domain size and an increase in domain density at low dopant concentrations. A development of the 'undulatory' character of the walls of the domain walls at moderate concentrations, indicating pinning of the domain walls. However, the electro-neutrality of PZTs is ensured by the appearance of oxygen vacancies that make the material non-stoichiometric (**Fig.I.19**). Acceptor dopants lead to ageing of the PZT's properties and therefore to the presence of an internal field. They also cause an increase in: the mechanical quality factor, the coercive field and the conductivity.

And a decrease in: permittivity, coupling coefficients, dielectric losses and ceramic grain size **[16]**.

I.4.2.3. Substitution by an ion with a higher valency than the substituted ion

PZT materials doped with donors are said to be 'soft' because they are easily depolarized and are little or not affected by ageing. However, the excess positive charge provided by the donor dopants is compensated for by cationic vacancies. Donor dopants lead to the development of regular domain patterns with increasing concentration, including: micrometer-sized domains and complete domain structures characterized by a strong and broad dependence of dielectric response to temperature.

Donor dopants generally lead to an increase in: dielectric loss permittivity, coupling coefficients and elastic compliance. There is also a decrease in: mechanical quality factor, conductivity, coercive field and Curie point.

The choice of dopant therefore depends mainly on the intended application of the material.

When an acceptor replaces a higher valency ion, the oxygen vacancies created are often mobile thanks to a jump mechanism that is easy for oxygen atoms. This mobility of the oxygen vacancies stabilizes the domain walls anchored in these vacancies, which explains the reduction in mechanical losses.

In the case of a donor, A-site vacancies are created. The distance between these gaps and the A sites is so great that jumping is forbidden without energy input. Furthermore, the movement of domain walls, which is limited in the case of materials doped by acceptors, is not affected in the case of those doped by donors.

(**Fig.I.19**) is an explanatory diagram of the mobility of the oxygen vacancies in the doped material **[16]**.

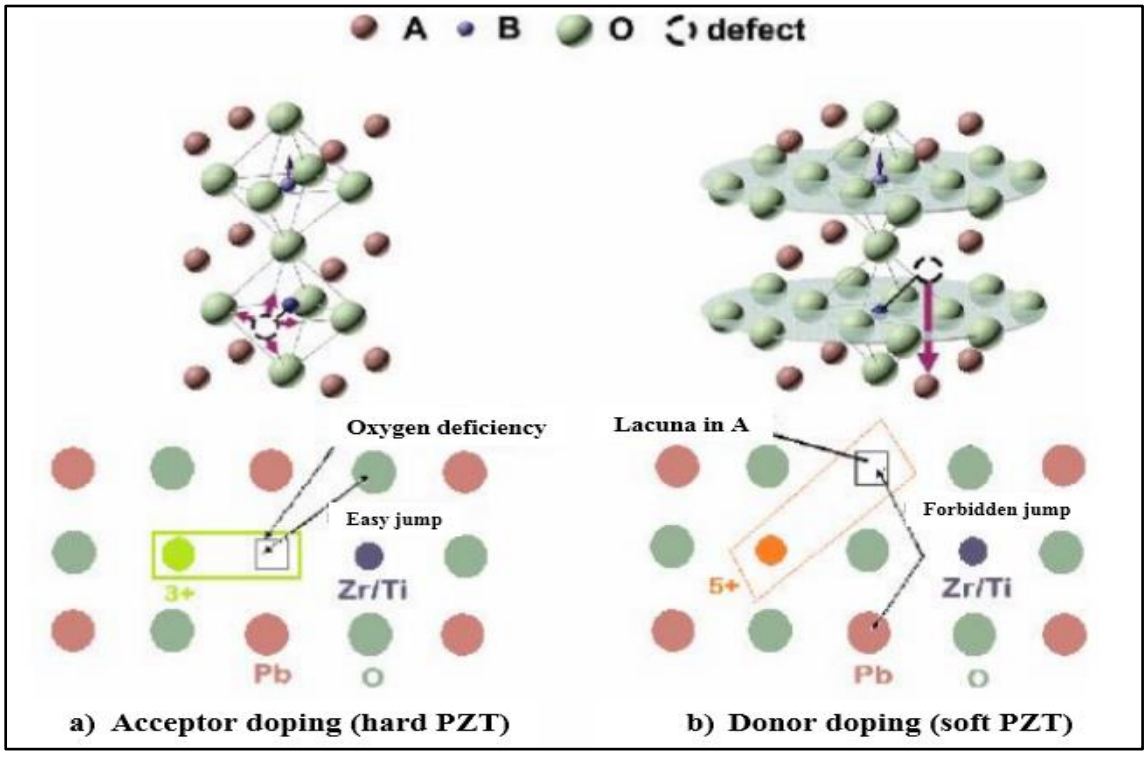

Figure I.19: Defects created in the PZT lattice after substitution by: (a) acceptor ions (left) (b) donor ions (right) [17].

I.5. Applications of piezoelectric materials

There are many applications for piezoelectric ceramics, which fall into six categories:

- Piezoceramic transmitters and receivers for hydro- and aeroacoustics applications such as sonar or level detectors.
- Transducers for ultrasound equipment for medical use (dental scalers, scalpels and inhalers) or industrial use (cleaning, drilling, welding).
- Piezoelectric actuators for fuel injection systems, vibration damping and other applications.
- High-voltage pulse generators for gas lighters, cigarette lighters and explosives fuses.
- Sensors such as microphones, hydrophones, remote control and accelerometers.
- Positioning devices such as actuators for positioning mirrors and controlling small mechanical movements **[3]**.

I.6. Previous works

Many researches on different PZT ceramic materials have been carried out **[18-22]** in the laboratory.

This research has been based on the synthesis and characterization of new and unstudied PZT ceramic materials. This can be achieved by adjusting the Zr/Ti ratio which determines the ratio of the quaternary and rhombic phase near the MPB, and by grafting the material with different cationic substituents and substitution at the A and B site of the perovskite to optimize the physical properties of PZT.

Research activity in this area is as important as ever, with research being published in many journals of interest **[23]**.

The current work is a continuation of similar studies previously conducted on ternary systems doped at the A and B site of perovskite **[18,23]** and the aim is to optimize the properties and performance of this system.

Bibliographic References

[1] A.Meklid **,** Elaboration, caractérisation et étude des propriétés diélectriques et électromécaniques d'un nouveau matériau de céramique de type Zirconate-Titanate de plomb (PZT)**,** Thèse de doctorat, Université Mohamed Khider-Biskra-Algérie,2018.

[2] R.K.Abdelli, Synthèse et caractérisation d'un matériau de la structure pérovskites à base plomb, Mémoire de Master, Université Mohamed Khider-Biskra- Algérie ,2018.

[3] K. Haddouf, Elaboration et caractérisation des céramiques piézoélectriques, Mémoire de Master, Université Mohamed Khider-Biskra- Algérie, 2018.

[4] C. Benhamideche, Thèse de Magister, Université de Constantine- Algérie, 1998.

[5] F. Kahoul, Elaboration et caractérisation de céramiques PZT dopé et détermination de la frontière morphotropique (FMP), Thèse de doctorat, Université Mohamed Khider-Biskra- Algérie, 2013.

[6] R.Boudraa et A.Bordjah, Etudes diélectrique, optique et photocatalytique de $BaTiO_3$, Mémoire de Master, Université Abderrahmane Mira - Béjaïa - Algérie ,2020.

[7] M.Abba, Synthèse, caractérisation et étude Des propriétés Piézo-électriques des céramiques de type PZT: $Pb_{1-y}La_y[Zr_xTi_z(Mo_{1/3}In_{2/3})_{1-(x+z)}]_{1-y/4}O_3$, Thèse de doctorat, Université Mohamed Khider-Biskra-Algérie, 2013.

[8] P. Tomar, P.kumar , N.Ali , S.Kumar , T.Musharraf , P.Kumar, Conversion of noise pollution to electrical energy, International Journal of Advance Research in Science and Engineering (IJARSE), Vol. 5, No. 03, March 2016 , p514-522.

[9] M.Khacheba, Elaboration et caractérisation diélectrique de céramiques de formule : $A_x(Y_{0.5},Na_{0.5})_{1-x}[(Zr_{0.05},Ti_{0.95})_{0.97}(Al_{1/3},Zn_{1/2},W_{1/3})_{0.03}]$ (A=Pb, Ba), Thèse de doctorat, Université Mohamed Khider-Biskra-Algérie, 2023.

[10] F.Benabdallah, Evolution des propriétés diélectriques, ferroélectriques et électromécaniques dans le système pseudo-binaire $(1-x)BaTi_{0.8}Zr_{0.2}O_3$ $_xBa_{0.7}Ca_{0.3}TiO_3$ / Corrélations structures et propriétés, Thèse de doctorat, Université Bordeaux 1-Sfax-Tunisie, 2013.

[11] F.Z.Fadil, Synthèse et Caractérisation des Matériaux PT : Mg et LN : Mg/Ho en vue de Fabrication de Fibres Cristallines, Thèse de doctorat, Université de Lorraine - Français, 2012.

[12] A.Meklid, Étude de la transition de phase de la solution solide de céramiques piézoélectrique dans le système ternaire : (0.80-x)Pb($Cr_{1/5}$,$Ni_{1/5}$,$Sb_{3/5}$)O_3-x$PbTiO_3$-0.20$PbZrO_3$, Thèse de magistère, Université De Kasdi Merbah -Ouargla - Algérie,2011.

[13] R.Bounouioua, Les effets de préparation sur les propriétés diélectriques des céramiques du type $BaTiO_3$ + x % mole Fe_2O_3, Mémoire de magister, Université Mentouri - Constantine -Algérie, 2006.

[14] Z. HE, J. MA and R. ZHANG, Investigation on the microstructure and ferroelectric properties of porous PZT ceramics, Ceramics International, Vol.30, No. 7, 2004, p1353-1356.

[15] L.Boussouf, Synthèse et caractérisations d'une céramique electrotechnique du type : CAO $Al_2O_3$6SiO_2 - $Al_2O_3$2SiO_2.H_2O -SiO_2, Thèse de magistère, Université Badji Mokhtar -Annaba- Algérie,2009.

[16] L.Lebssisse, Synthèse, étude structurale et morphologique des nouveaux matériaux en céramique, Mémoire de master, Université Kasdi Merbah - Ouargla - Algérie,2016/2017.

[17] Z.Necira**,** Étude de système quaternaire x$PbZrO_3$-y$PbTiO_3$- zPb($Mg_{1/3}$, $Nb_{2/3}$)$_{1/2}O_3$-zPb($Ni_{1/3}$,$Sb_{2/3}$)$_{1/2}O_3$ près de la frontière morphotropique de phase(FPM), Thèse de doctorat, Université Mohamed Khider-Biskra-Algérie,2018.

[18] A. Meklid, S.E. Hachani, Z. Necira, H. Menasra, M. Abba, A. Boutarfaia, Phase structure, microstructure and electrical properties of PCNS–PZ–PT ternary ceramics near the morphotropic phase boundary, Appl. Phys. Mater. Sci. Process, Vol. 126, No.32 ,2020.

[19] A. Boutarfaia, Study of the solid state reaction and the morphotropic phase boundary in Pb(Zr, Ti)O_3-Pb($Fe_{1/5}$, $Ni_{1/5}$, $Sb_{3/5}$)O_3 ceramics, Ceramics International, Vol. 27, No.1, pp. 91-97, 2001.

[20] N. Abdessalem, A. Boutarfaia, Effect of composition on the electromechanical properties of $Pb[Zr_x Ti_{(0.9-x)} (Cr_{1/5}, Zn_{1/5}, Sb_{3/5})_{0.1}]O_3$ ceramics, Ceramics International, Vol. 33, No.2, pp. 293-296, 2007.

[21] N. Abdessalem, A. Boutarfaia, M. Abba, Z. Necira, L'effet de l'addition de Nd^{3+} sur les propriétés diélectriques du système $Pb[Zr_{0.45}Ti_{0.45}(Zn_{1/3}, Sb_{2/3})_{0.1}]O_3$, Revue des Sciences Fondamentales et Appliquées, Vol. 3, No. 2, pp.1-7, 2011.

[22] A. Meklid, A. Boutarfaia, The effects of sintering temperature and titanium ratio on structural and electrical properties of new PZT-CNS ceramics. Model. Measur. Control C. Vol. 79, pp. 1-5, 2018 .

[23] A.Ksouri, A.Meklid, Z.Necira, S.E. Hachani, S.Bouzidi, A.Khiouani, H.Khemakhem, Impact of Sm_2O_3 doping on PZT-PMI-PZS ternary ceramics: Phase structure, microstructure, and dielectric characteristics, Ceramics International, Vol. 49, No.23, pp. 39223-39231, 2023.

Chapter II

Experimental Techniques

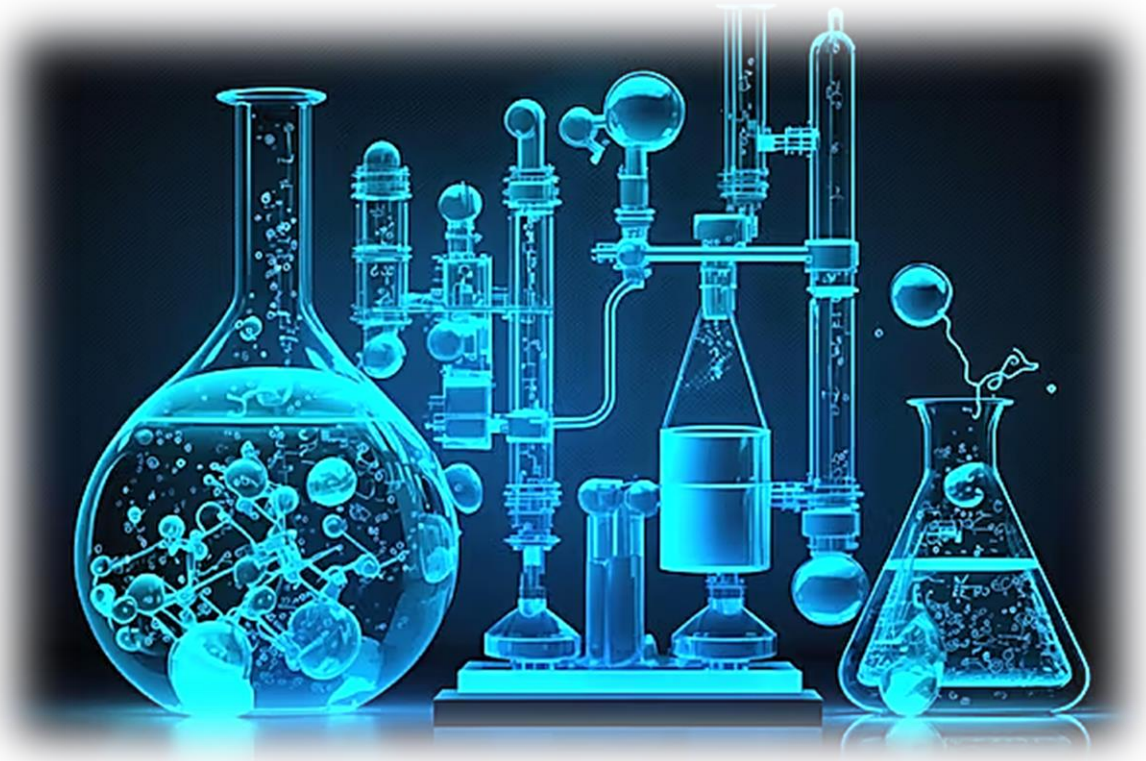

II.1. Introduction

This chapter begins by describing the synthesis and shaping techniques used to prepare ceramics with a perovskite structure. It then describes the physico-chemical characterization techniques used to explore their chemical, structural and microstructural properties.

The technique chosen to form a solid depends not only on its composition, but also on the state in which it is to be used (grain size, porosity, surface finish, homogeneity, etc.). Powder preparation is an important stage in shaping processes. The aim is to obtain a powder which, on the one hand, produces the desired microstructure, generally dense and homogeneous, during shaping and, on the other hand, ensures satisfactory densification during sintering. There are two main ways of manufacturing ceramics:

- The solid route (ceramic method).
- The liquid or chemical route.

We are interested here in the ceramic method, which is the most widely used in the laboratory and industry because of its simplicity and low cost **[1,2]**.

II.2. Ceramic method

The ceramic method (CM) is the simplest method for producing ceramic materials. This method involves reacting a reaction mixture made up of different powdered precursor solids at high temperature (possibly under a reactive atmosphere).

The ceramic method is characterized by the fact that the solids are not heated to their melting temperatures and the reactions take place in the solid state. Such a reaction only occurs at the interface between the grains of the solids. Once the surface layer has reacted, the reaction can only continue if the reactants diffuse from the core towards the interface. Increasing the temperature accelerates the reaction because diffusion through the solid occurs more rapidly than at ordinary temperatures **[3]**.

(**Fig.II.1**) summarizes the advantages and disadvantages of the ceramic method **[4,5]**.

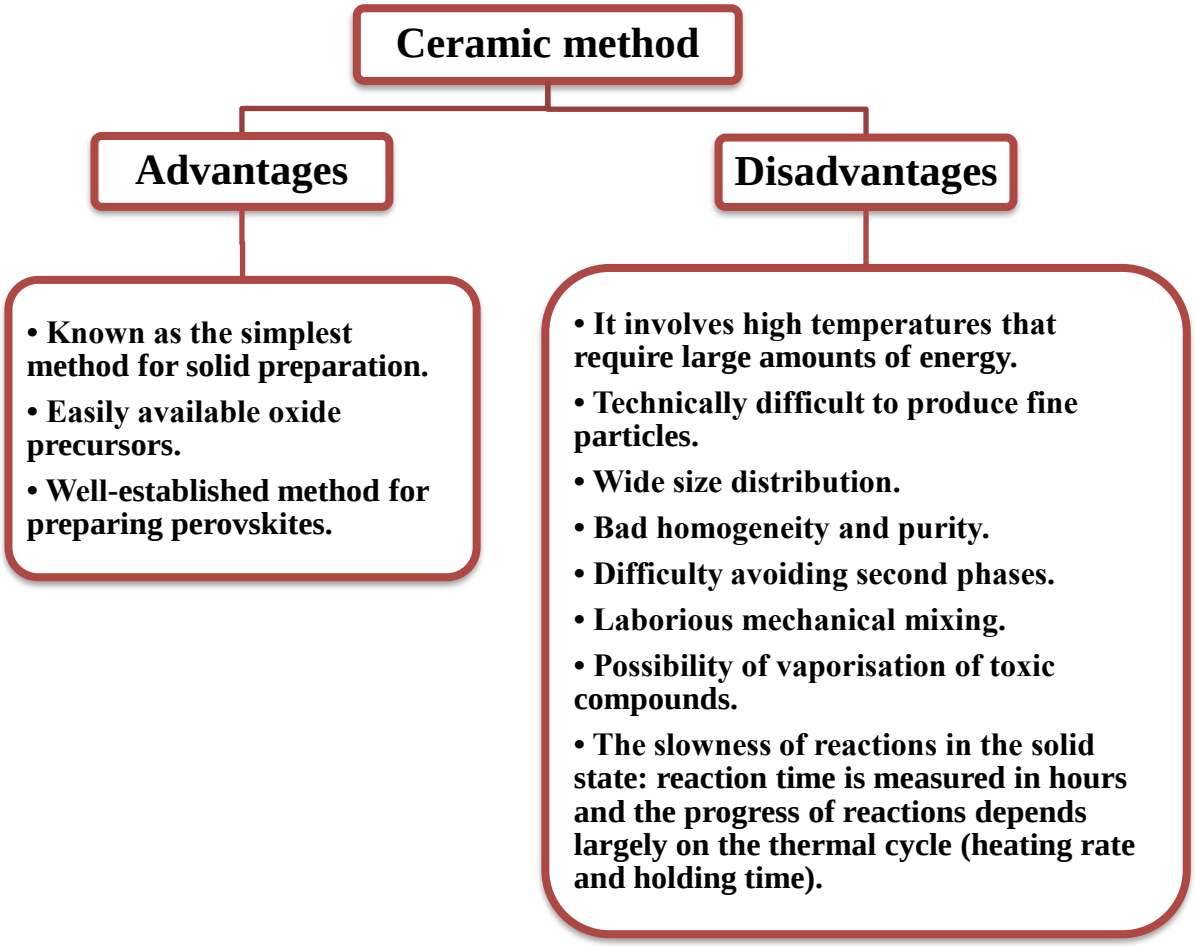

Figure II.1: Advantages and disadvantages of ceramic method.

To avoid these disadvantages, it is important that the starting materials are well ground to reduce particle size and that they are very well mixed to have maximum contact surface and reduce the diffusion distance of the reagents **[4]**.

II.3. Experimental procedure

II.3.1. Starting products

Our **PCZT-FZS** solid solution is prepared from a mixture of starting products (base oxides and dopants).

II.3.1.1. Basic products

The basic oxides used in the synthesis of our samples are: PbO, TiO_2, ZrO_2, whose purity levels are given in (**Tab.II.2)**.

- **Lead oxide PbO**

Lead(II) oxide, also called lead monoxide, is the inorganic compound with the molecular formula PbO. It occurs in two polymorphs:

The litharge, PbO with tetragonal structure, exists in a reddish alpha form up to 489°C; it then transforms into a yellow beta form (massicot) of orthorhombic structure, which is stable at high temperatures. Lead oxides are produced industrially by thermal processes in which the lead is directly oxidized by air **[2,6]**.

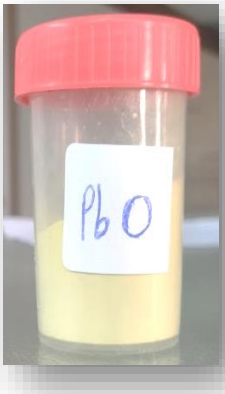

Figure II.2: Lead monoxide powder.

Table II.1: The main crystallochemical characteristics of lead monoxide PbO.

Species	Formule	Colour	System	Mesh parameters (Å)
litharge	α-PbO	red	Quadratique	a = 3.960 c = 5.010
massicot	β-PbO	yellow	Orthorhombique	a = 5.476 b = 5.486 c = 4.743

- **Zirconium dioxide ZrO_2**

Zirconia (zirconium dioxide) is white in color. It has good hardness, good resistance to thermal shock and corrosion, low thermal conductivity and a low coefficient of friction. It has a fluorite-type structure.

The lattice is monoclinic with parameters a = 5.14Å, b = 5.20Å and c = 5.21Å, β = 80°45'. Its melting temperature is 2700°C **[8]**.

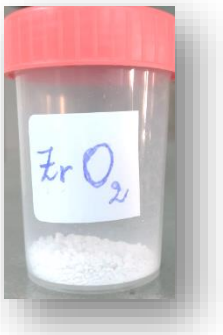

Figure II.3: Zirconium dioxide powder.

➢ **Titanium dioxide TiO_2**

It is a white powder when cold and yellow when hot. It has a melting point of 2000°C and a boiling point of 3000°C. Rutile TiO_2 has a quadratic structure and parameters a= 4.59 Å and c= 2.96 Å **[2]**.

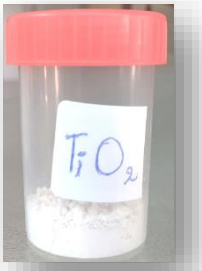

Figure II.4: Titanium dioxide powder.

II.3.1.2. Dopants

Lead zirconate titanate (PZT) materials are widely used in a variety of applications, but rarely in simple chemical formulations. They are often modified by the introduction of substitutional elements (dopants) in the A-sites or B-sites of their ABO_3 perovskite structure.

In our work, we will dope in A-site with calcium carbonate $CaCO_3$, and B-site with iron oxide Fe_2O_3, zinc oxide ZnO and antimony trioxide Sb_2O_3.

➢ **Calcium carbonate $CaCO_3$**

Calcium carbonate which is a white powder has been widely used in industry due to its stability and economy. It has a melting point of 1339°C. Calcium carbonate has three types of crystalline polymorphism, calcite, aragonite and vaterite, each with different properties.

The calcite crystal structure is trigonal, and Aragonite is orthorhombic, Vaterite is composed of at least two different coexisting crystallographic structures **[7,9]**.

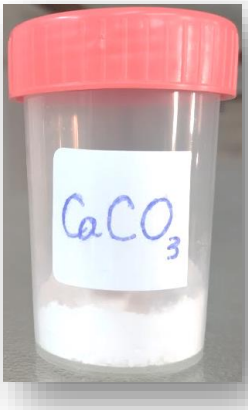

Figure II.5: Calcium carbonate powder.

- **Iron oxide Fe_2O_3**

It is obtained by heating FeO (OH) to a temperature of 200°C and is reddish-brown in color. It is used in low-temperature pastes and enamels **[8]**.

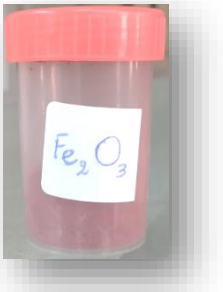

Figure II.6: Iron oxide powder.

- **Zinc oxide ZnO**

Zinc oxide is a white powder and is a versatile material, occupying an important place in a wide range of applications. Structurally, zinc oxide is a wurtzite crystal **[5]**.

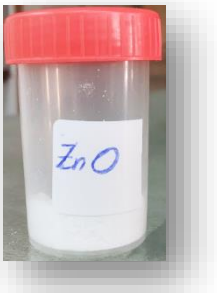

Figure II.7: Zinc oxide powder.

- **Antimony trioxide Sb_2O_3**

White powder, which transforms into Sb_2O_5 in the presence of oxygen, with a melting temperature of 656°C, and an orthorhombic or cubic structure **[10]**.

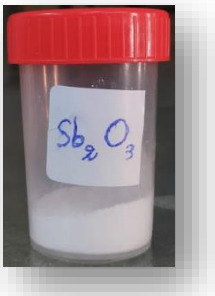

Figure II.8: Antimony trioxide powder.

II.3.2. Sample preparation method

In this study, PZT-type ceramics were synthesized from a mixture of oxides. The starting compounds were commercial products: PbO, ZrO_2, TiO_2, $CaCO_3$, Fe_2O_3, ZnO and Sb_2O_3.

(**Tab.II.2**) summarizes the characteristics of the starting materials. These compounds are pure products 'for analysis' for which the level of residual impurities does not affect the physical properties in a remarkable way.

Table II.2: Characteristics of starting products.

Starting products		**Molar mass (g/mol)**	**Purity (%)**
Basic products	PbO	223.200	99.0
	ZrO_2	123.222	99.0
	TiO_2	079.870	99.0
Doping products	$CaCO_3$	100.090	99.6
	Fe_2O_3	159.690	99.6
	ZnO	081.370	99.6
	Sb_2O_3	291.498	99.6

The different stages in the synthesis method using this route are illustrated in (**Fig.II.9**).

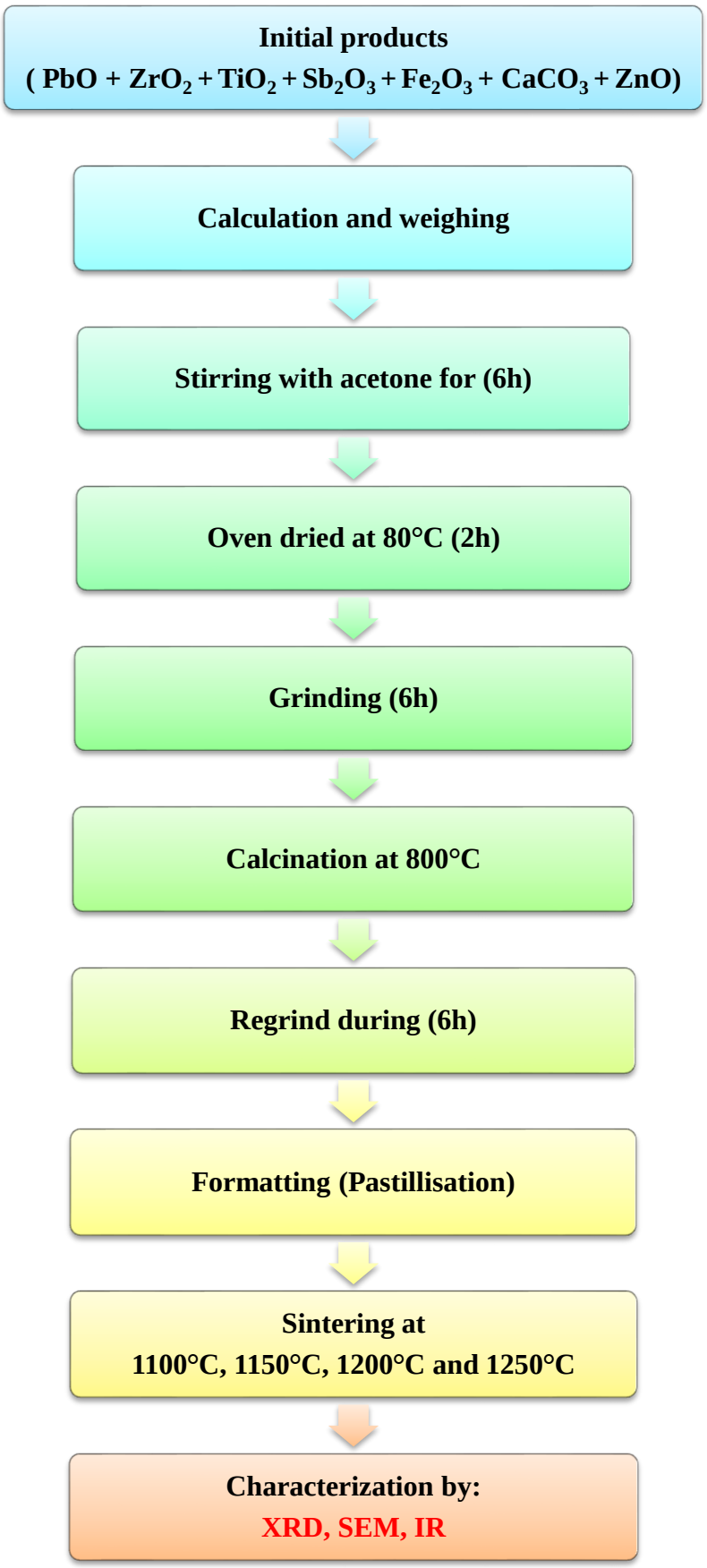

Figure II.9: The main stages in the preparation of PZT ceramics.

The sample preparation process can generally be described in four main stages: weighing and stirring, grinding, calcination and sintering.

II.3.2.1. Weighing and stirring

This is an essential phase in the ceramic manufacturing cycle. It is also during this operation that a uniform distribution of precursors is obtained. The oxides are weighed in stoichiometric proportions using a balance with a precision of ± 0.0001 g.

The powders are then homogenized using a magnetic stirrer in the presence of acetone for 6h ($T_{boiling}$= 56.05°C).

It should be noted that the choice of acetone was based on the fact that it has a low evaporation point and therefore dries quickly **[5]**.

Figure II.10: Stirring in acetone medium.

II.3.2.2. Oven drying

This stage consists of drying the mixture obtained at a temperature of 80°C for two hours in an oven until the acetone evaporates. The compounds are again in powder form.

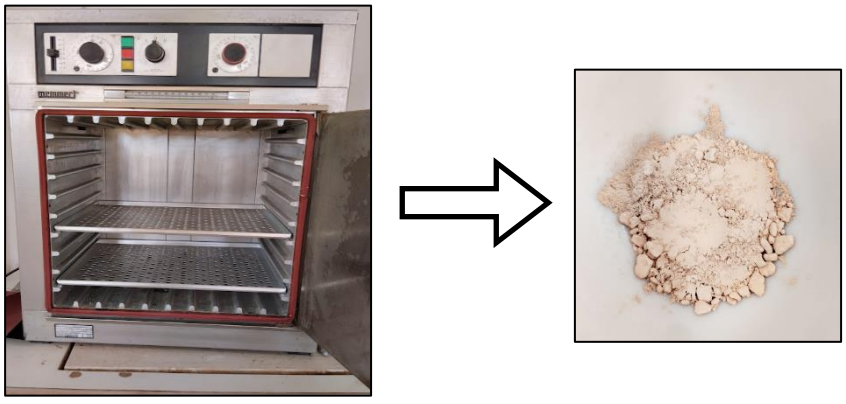

Figure II.11: Oven drying.

II.3.2.3. Grinding

Grinding is carried out in a glass mortar for six hours. This produces fine particles, which encourages phase formation by faster solid/solid diffusion.

Figure II.12: A glass mortar (grinding).

II.3.2.4. Calcination

Heat treatment, also known as calcination, is carried out at around 800°C in a programmable furnace (Nabertherm) at a heating rate of 2°C/min. Calcination is used to form the perovskite phase. To this end, the samples are placed on a ceramic plate and subjected to a thermal cycle during which they react by solid-phase diffusion to form the desired phase **[2]**.

Figure II.13: The furnace used in the calcination process and the samples before and after calcination.

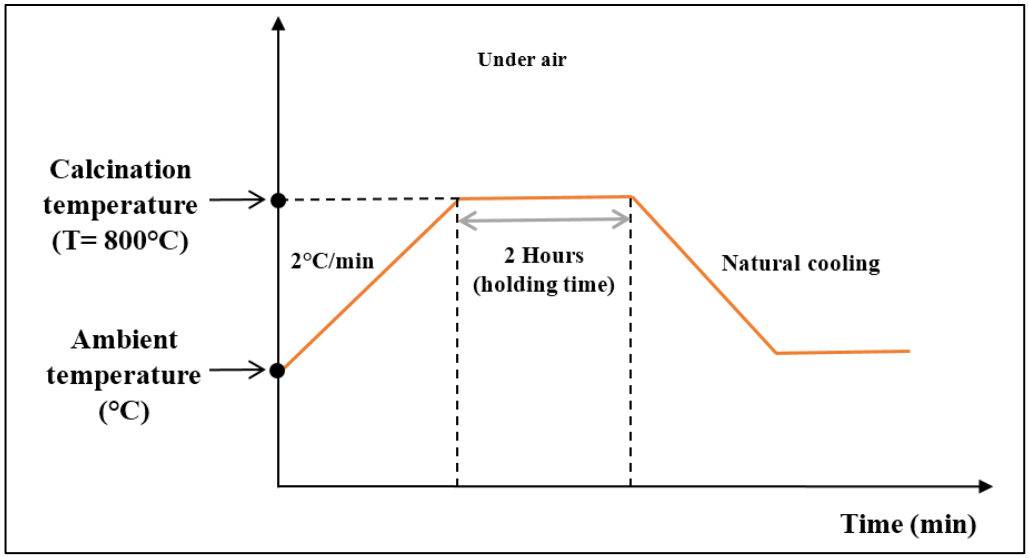

Figure II.14: Calcination thermal cycle and furnace used.

II.3.2.5. Regrinding

The aim is to separate the agglomerates, homogenise the powder, which has generally not reacted uniformly during the grinding, and reduce the particle size in order to increase the powder's reactivity. This grinding is carried out under identical conditions to the first grinding **[5]**.

Figure II.15: Regrinding after calcination.

II.3.2.6. Formatting

Compositions with a mass of 1.1 g are compacted at 3000 kg/cm^2 using a manual press (**Fig.II.16**) with a mould that gives the pellets a cylindrical shape.

The diameter of the pellets is fixed (13 mm) and their thickness varies according to the force applied **[11]**.

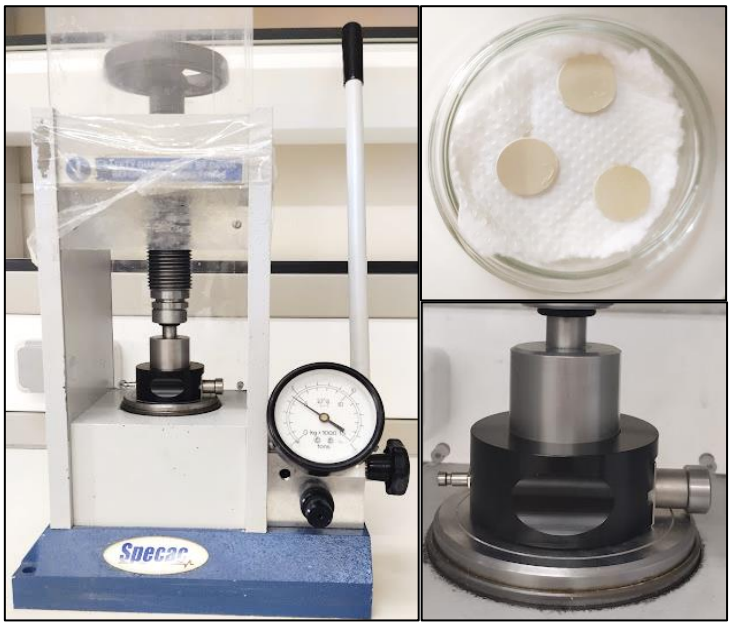

Figure II.16: The press and mold used to prepare the pellets.

II.3.2.7. Sintering

- **Definition**

Sintering can be defined as the consolidation by the action of heat of a more or less compact granular agglomeration, with or without fusion of one or more of its constituents. It minimises the surface free energy of a solid **[5]**.

- **Sintering conditions**

The sintering of samples is a delicate operation, depending essentially on two parameters, the temperature (kinetic and palpy) and the sintering atmosphere. These two parameters have a direct influence on the density, grain size and compositional homogeneity of the material.

The main problem encountered when sintering PZT ceramics is the volatility of lead oxide, which is highly volatile [$T \geq 900°C$], so the amount of $PbZrO_3$ powder added to minimise PbO volatilisation was controlled for each sintering operation. Thus, the mass loss or excess was controlled by weighing the sample before and after sintering, Noting that it should not exceed a value of $\Delta m \leq 2\%$. The optimum sintering temperature corresponds to the evaporation-decondensation equilibrium of PbO .

In fact, the samples to be sintered are placed on a small alumina crucible, avoiding contact between the sintered pellets, the crucible is then placed on a sheet of alumina within which a quantity of $PbZrO_3$. Finally, the crucible is covered with a larger one as shown in (**Fig.II.17**), and the whole assembly is placed in the furnace at temperatures of 1100, 1150, 1200 and 1250°C according to the thermal cycle shown in (**Fig.II.18**) **[5,11-14]**.

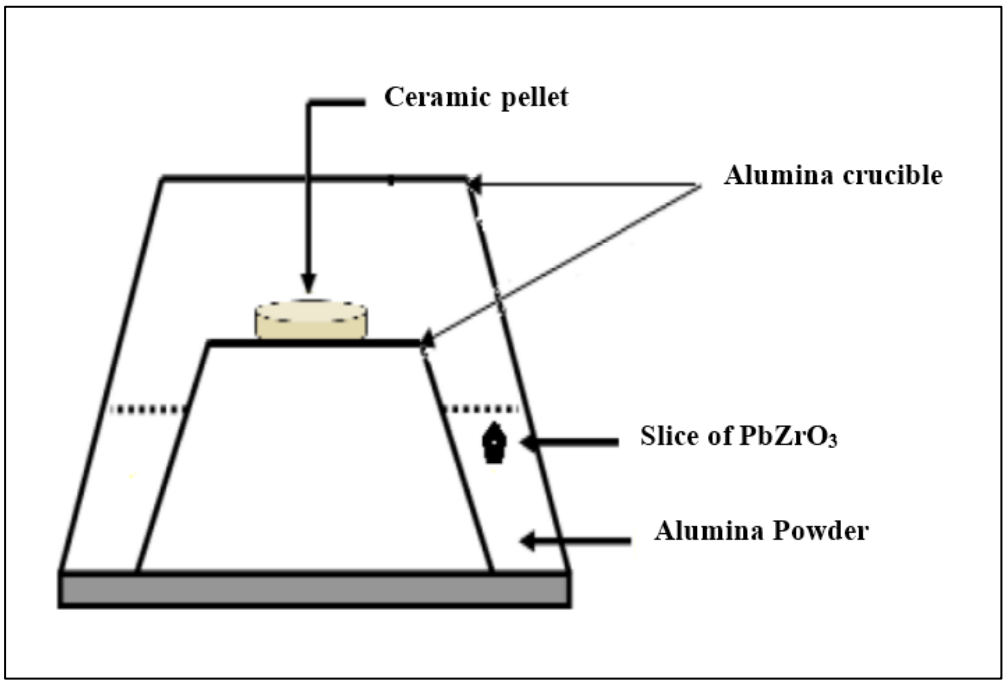

Figure II.17: Sintering device.

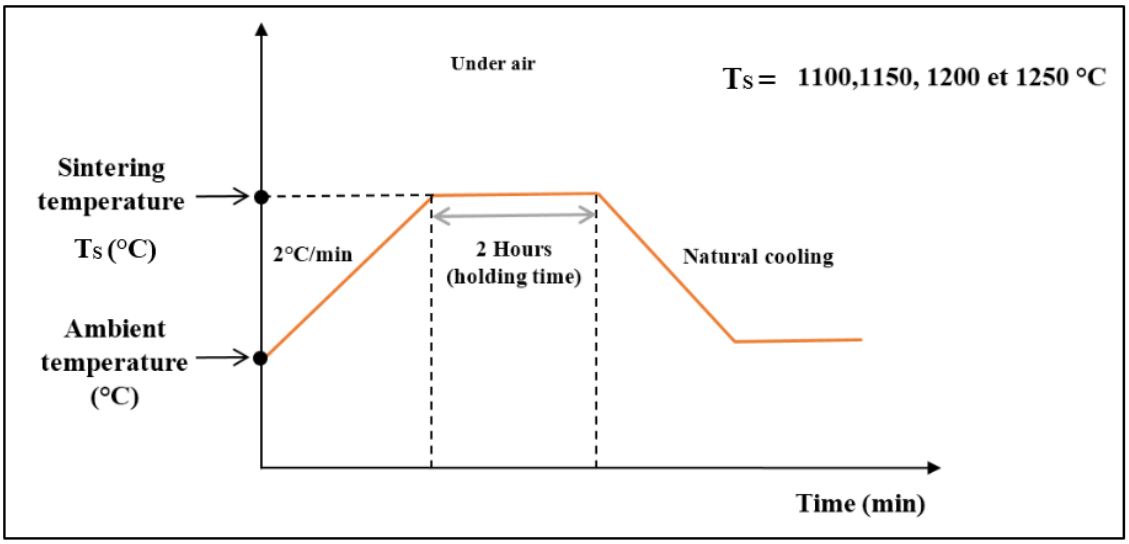

Figure II.18: Sintering thermal cycle.

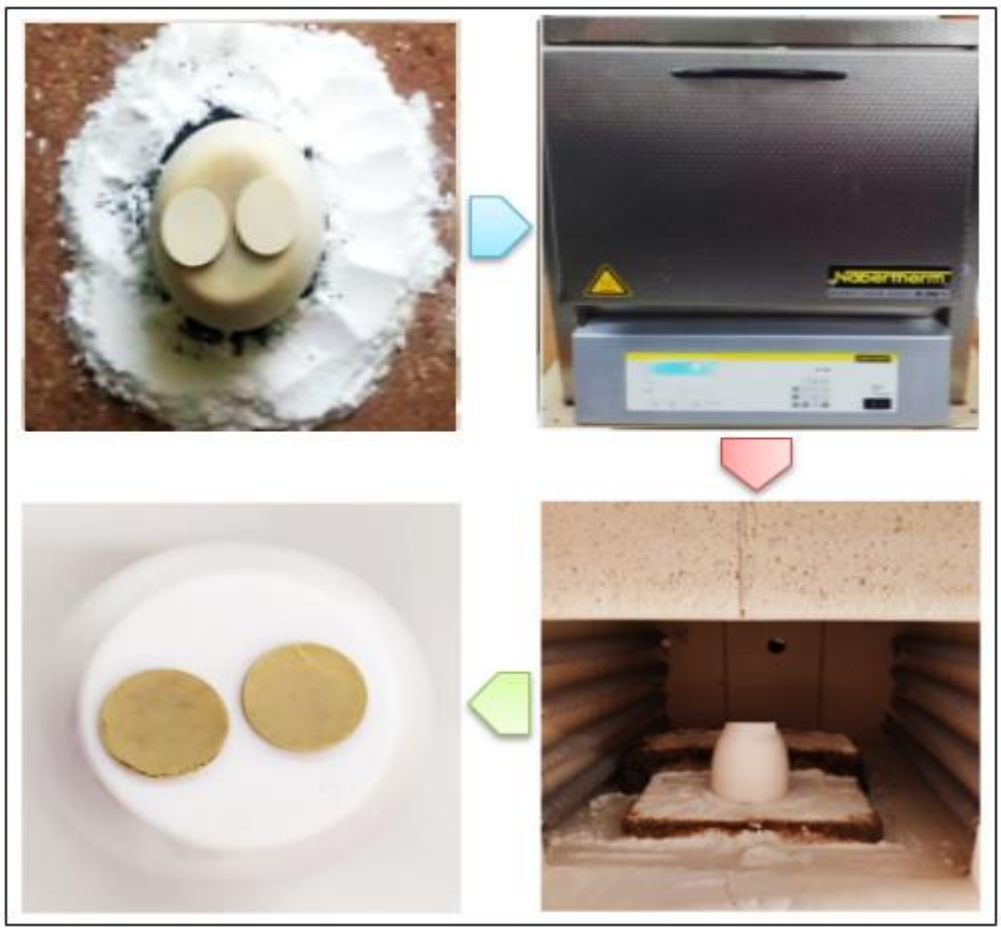

Figure II.19: Sintering stages.

II.4. Experimental characterization techniques: Analysis and equipment

II.4.1. Measuring density (d)

The density of ceramics is defined as the mass per unit volume. The quality of the material increases as the density increases, and the density increases as the sintering temperature increases **[2,15]**. The structural and physical properties of a ceramic are related to its density.

In order to optimize the sintering temperature for the samples selected in this study, density measurements were carried out based on geometric measurements (diameter and thickness) on each pellet for the five samples sintered at different temperatures (1100, 1150, 1200, and 1250°C). These measurements were made using an electronic caliper.

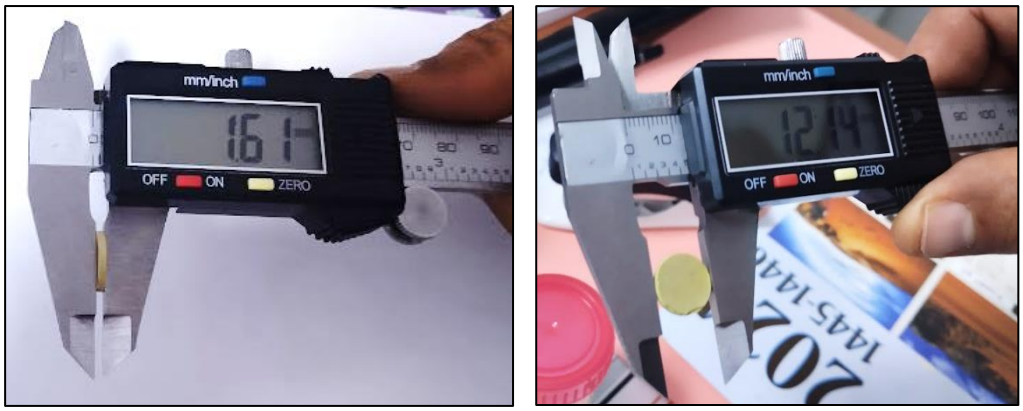

Figure II.20: Electronic caliper.

The density (d) is calculated by the formula:

$$\mathbf{d} = \frac{\mathbf{m}}{\boldsymbol{\pi}(\frac{\boldsymbol{\phi}}{\mathbf{2}})^{\mathbf{2}}\mathbf{e}} \ldots\ldots\ldots\ldots\ldots (\mathbf{II.1})$$

Where:

m: Mass of the pellet (g).

ϕ: Pellet diameter (cm).

e: Pellet thickness (cm).

II.4.2. Measuring porosity (P)

The study of porosity as a function of temperature has many advantages, the most important of which is to obtain ceramic samples that are even less porous, because their mechanical properties depend on their porosity. This is a critical parameter in PZT ceramic technology **[2]**. Porosity is calculated as follows:

$$\mathbf{P} = \mathbf{1} - \mathbf{D} \ldots\ldots\ldots\ldots\ldots (\mathbf{II.2}) \qquad \text{Where} \quad \mathbf{D} = \frac{\mathbf{d_{exp}}}{\mathbf{d_{theo}}} \ldots\ldots\ldots\ldots\ldots (\mathbf{II.3})$$

$$\mathbf{d}_{exp} = \frac{\mathbf{m}}{\boldsymbol{\pi}(\frac{\boldsymbol{\phi}}{\mathbf{2}})^{\mathbf{2}}\mathbf{e}} \ldots\ldots\ldots\ldots\ldots (\mathbf{II.4}) \quad ; \quad \mathbf{d}_{theo} = \frac{\mathbf{MZ}}{\mathbf{VN}} \ldots\ldots\ldots\ldots\ldots (\mathbf{II.5})$$

With:

$\mathbf{d_{exp}}$: Experimental density of the composition (g/cm^3).

$\mathbf{d_{the}}$: Theoretical density of the composition (g/cm^3).

M: Molar mass of the sample.

Z: Number of form units per mesh.

N: Avogadro number.

V: Mesh volume.

II.4.3. Crystal structure analysis by XRD

X-ray diffraction is considered to be a key technique for resolving crystalline structures due to its high sensitivity to changes in the elemental lattice of crystals or polycrystalline materials.

Sample preparation seems to be one of the essential parameters for obtaining good quality, reproducible results, as the three main pieces of information obtained from diffraction data are influenced by the sample **[2,16]**:

- The position of the lines.
- The intensity of the lines.
- The shape of the lines.

X-ray diffraction by crystals was discovered by Friedrich, Knipping and von Laue in 1912 and is based on Bragg's law. (**Fig.II.21**) illustrates the principle of Bragg's law. A crystal made up of atomic planes separated by a distance 'd' receives electromagnetic radiation of wavelength 'λ'. X-ray diffraction measurements were carried out and the positions of the diffracted planes are given by Bragg's relation as follows **[5,17]**:

$$\mathbf{2d \sin\theta = n\lambda} \ldots\ldots\ldots\ldots\ldots (\mathbf{II.6})$$

With:

d: inter-reticular distance between the planes referenced by the Miller indices (h,k,l) .

λ: X-ray wavelength.

θ: diffraction angle.

n: diffraction order.

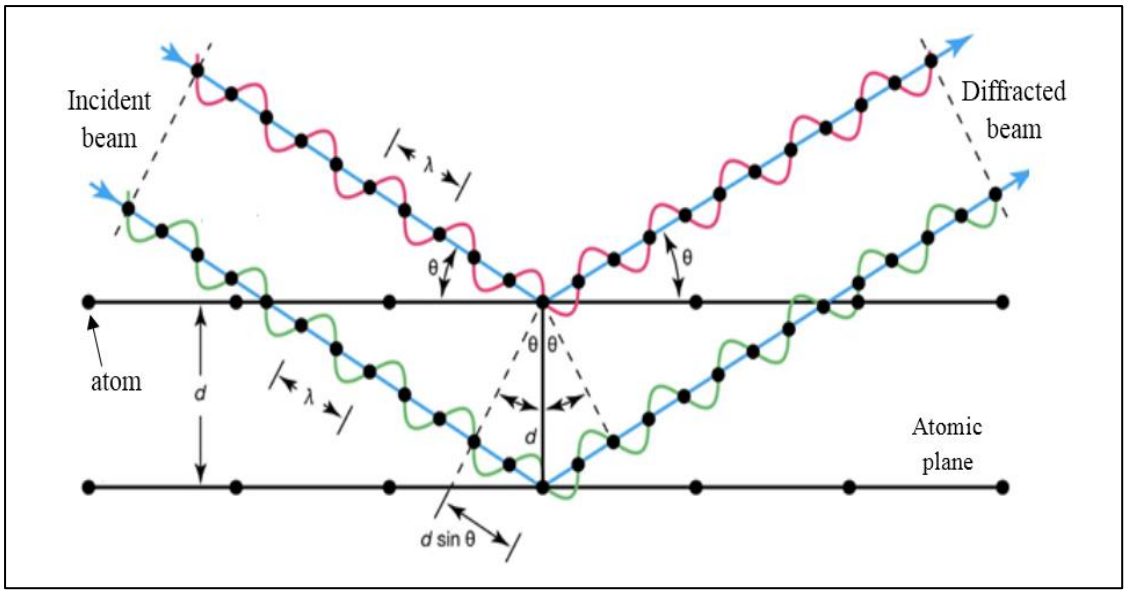

Figure II.21: Bragg's law principle.

The diffracted beam is transmitted as a signal which is amplified and recorded as a diagram I =f (2θ), (**Fig.II.22**) **[18]**.

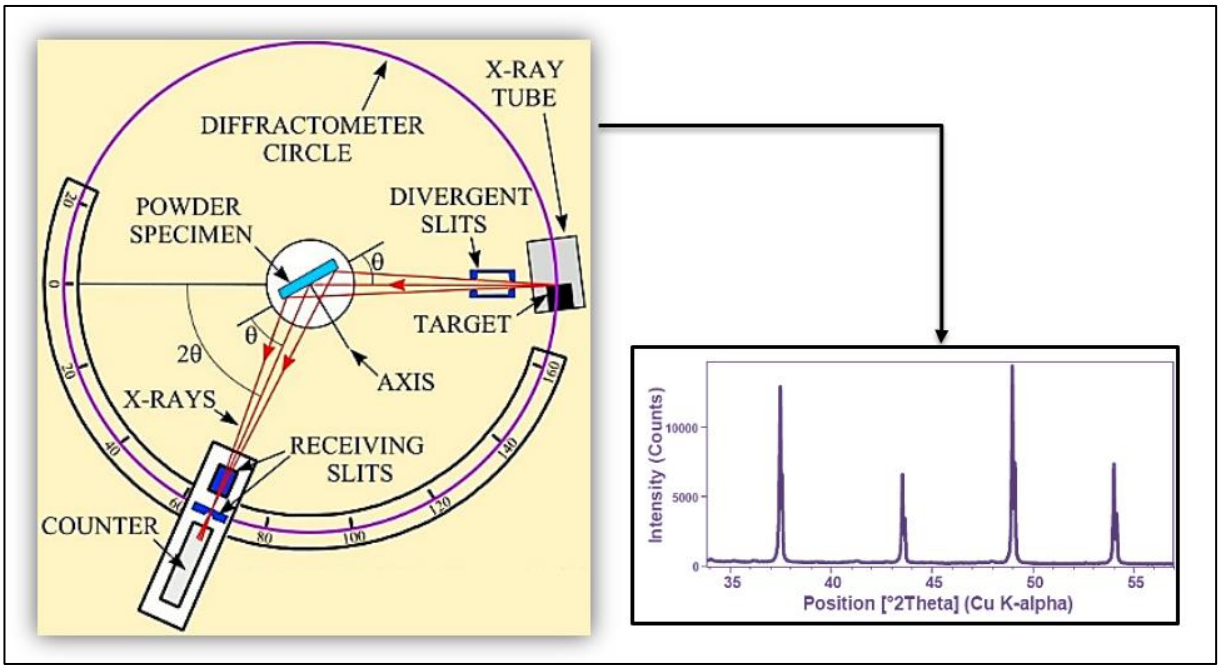

Figure II.22: Powder diffractometer principle.

- **BRUCKER-AXS type D8 ADVANCE diffractometer:**

The radiocrystallographic analysis of the samples at room temperature was carried out using the BRUCKER-AXS diffractometer type D8 ADVANCE which is installed in the XRD and SEM laboratory at the University of Biskra (**Fig.II.23**).

This diffractometer is characterized by X-rays that were produced from a Cu K_α radiation source having a wavelength λ=1.54 Å, with an accelerating voltage of 40KV and a current of 40 mA. Diffractograms are recorded at room temperature with 2θ between 10° and 90°. The software used to characterize the different lines is HighScore Plus **[2]**.

Figure II.23: BRUKER-AXS Diffractometer type ADVANCE D8.

II.4.4. Infrared spectroscopy (IR)

Infrared absorption (IR) (**Fig.II.25**) results from changes in the vibrational and rotational states of a molecular bond. It shows the presence of specific atomic groups in a given phase. We used the Fourier Transform Infrared Spectroscopy (FTIR) technique. The FTIR spectra were measured using an IR instrument (Shimadzu) operating in the range 400-4000 cm^{-1}, with a spectral resolution of 4 cm^{-1}. However, each sample was pelleted in potassium bromide with a proportion of 1 to 3 units by mass, the spectra obtained in the 4000 to 500 cm^{-1} range **[2].**

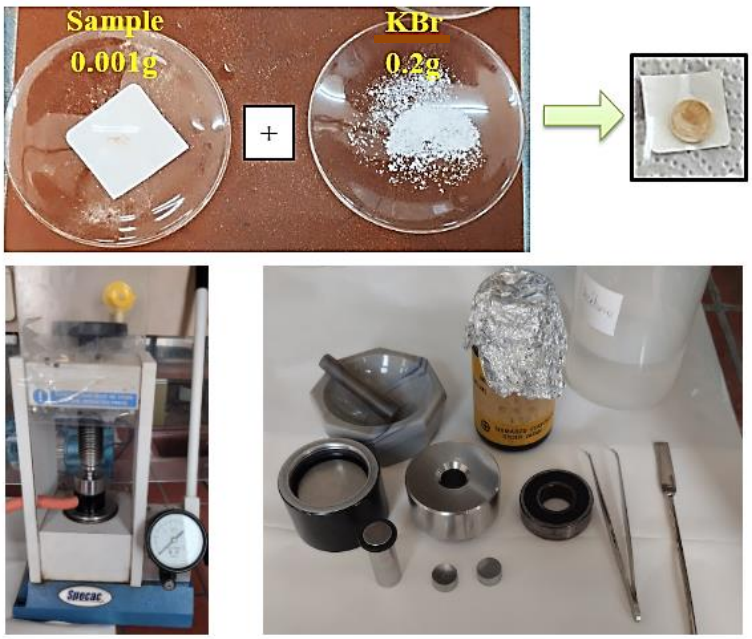

Figure II.24: IR Sample Preparation.

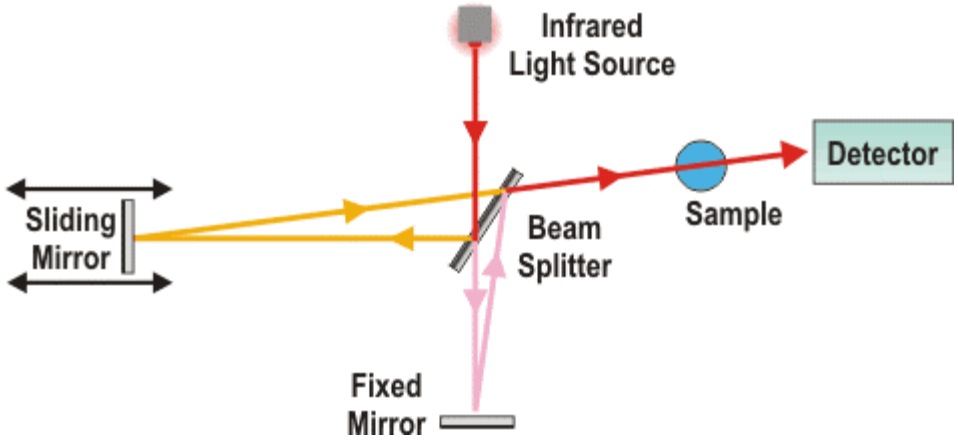

Figure II.25: Schematic diagram of the FTIR spectrophotometer and FTIR infrared spectrometer used.

II.4.5. SEM analysis

This technique is based on the detection of secondary electrons collected by bombardment of the sample. It provides a high-resolution image with a large depth of field. Scanning electron microscopy provides information on grain shape and size. This technique can be used to estimate the particle size distribution, the average grain size after sintering and to qualitatively assess the presence of porosity. (**Fig.II.26**) is a schematic cross-section of a scanning electron microscope.

The electron column is made up of all the elements used to obtain an electron beam focused on the sample **[8,18,19]**.

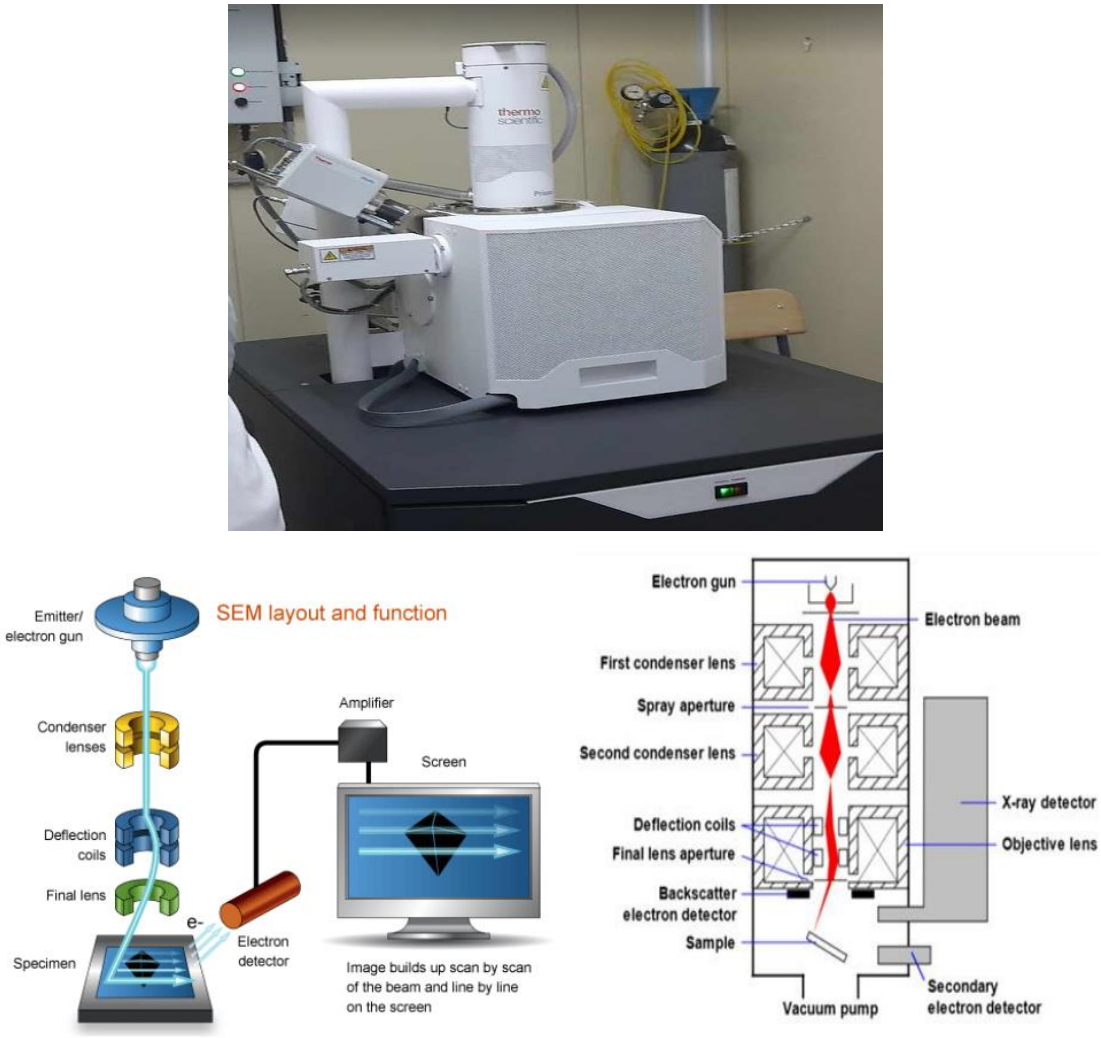

Figure II.26: Schematic of scanning electron microscope (SEM).

Bibliographic References

[1] H. Boureghda, N.Bouta , Synthèse et caractérisation des compositions fluoropérovskites de type PZT : (1-x) PZT - x SrF2 , Mémoire de Master, Université Mohamed Khider-Biskra-Algérie, 2020.

[2] A.Meklid **,** Elaboration, caractérisation et étude des propriétés diélectriques et électromécaniques d'un nouveau matériau de céramique de type Zirconate-Titanate de plomb (PZT)**,** Thèse de doctorat, Université Mohamed Khider-Biskra-Algérie, 2018.

[3] K.Benzida, I.Benkahla, Effet de Dopage par Le Lanthane sur Les Propriétés Morphologique d'Une Solution Solide de Type PZT, Mémoire de Master, Université Mohamed Khider-Biskra-Algérie, 2020.

[4] M.Abba, Synthèse, caractérisation et étude Des propriétés Piézo-électriques des céramiques de type PZT: $Pb_{1-y}\ La_y\ [Zr_x\ Ti_z\ (Mo_{1/3}\ In_{2/3})_{1-(x\ +z)}]\ _{1-y/4}\ O_3$, Thèse de doctorat, Université Mohamed Khider-Biskra-Algérie, 2013.

[5] R.K.Abdelli, Synthèse et caractérisation d'un matériau de la structure pérovskites à base plomb, Mémoire de Master, Université Mohamed Khider-Biskra- Algérie , 2018.

[6] D. S. Carr, Lead Compounds, Ullmann's Encyclopedia of Industrial Chemistry, Vol.20, 2000, pp.611-619.

[7] M. M. H. Al Omari, I. S. Rashid, N. A.Qinna, A. M.Jaber, A. A. Badwan, Calcium Carbonate, Profiles of Drug Substances, Excipients and Related Methodology, 2016, pp. 31-132.

[8] K. Megherbi, S.Ferhat , Influence de la température de frittage sur les propriétés structurales et physiques dans le système ternaire PLZT-FZS, Mémoire de Master, Université Mohamed Khider-Biskra-Algérie, 2019.

[9] W.Nagaki, N.Doki, M.Yokota, K.Yamashita, T.Kojima, T.Tanaka, Control of crystal size and morphology of calcium carbonate crystal polymorphism, Materials Science and Chemical Engineering ,Vol.9, No.4, 2021, pp.38-45.

[10] S.Zahi, Étude de nouveaux matériaux de céramiques dans le système quaternaire : $xPbZrO_3\text{-}yPbTiO_3\text{-}zPb\ [(Ni_{1/3},Sb_{2/3})(Mn_{1/3},Sb_{2/3})]_{1/2}O_3$, Thèse de doctorat, Université Mohamed Khider-Biskra-Algérie, 2010.

[11] H.Menasra. Influence de la température de frittage sur les propriétés structurales, diélectriques et piézoélectriques dans le système ternaire : $Pb_{0.95}$ $(La_{1-z}, Bi_z)_{0.05}[(Zr_{0.6}, Ti_{0.4})_{0.95}(Mn_{1/3}, Sb_{2/3})_{0.05}]O_3$, Thèse de doctorat, Université Mohamed Khider-Biskra-Algérie, 2015.

[12] M. Abba, Z. Necira, N. Abdessalem, A. Meklid, H. Menasra, A. Boutarfaia, Elaboration and dielectric characterization of a doped ferroelectric material type PZT, Journal of Fundamental and Applied Sciences, Vol. 5, No.2, 2013, pp. 210 -219.

[13] A.Megriche, M.Troccaz, Effects of Excess PbO Addition on the Properties of Ferroelectric Doped PZT Ceramics, Materials Research Bulletin, Vol.33, No.4, 1998, pp. 569-574.

[14] Z.Necira**,** Étude de système quaternaire $xPbZrO_3$-$yPbTiO_3$- $zPb(Mg_{1/3}, Nb_{2/3})_{1/2}O_3$-$zPb(Ni_{1/3},Sb_{2/3})_{1/2}O_3$ près de la frontière morphotropique de phase(FPM), Thèse de doctorat, Université Mohamed Khider-Biskra-Algérie, 2018.

[15] A.Boutarfaia, Investigations of co-existence region in lead zirconate-titanate solid solutions: X-ray diffraction studies, Ceramics International, Vol.26, No.6, 2000, pp.583-587.

[16] R. Zachariaz, J. Ilczuc, D. Bochenek, Influence of the technology conditions on the mechanical and dielectric properties of the PZT- base piezoceramics trasducers solid state phenomens, Vol.89, 2003, pp 303- 308.

[17] K. Bedoud, I. Rahmani, H. Meradi, H. Merabet, R. Graine, L'effet Thermique sur les Couches Minces du TiO_2 Déposé par la Méthode de Pulvérisation Cathodique, Proceeding of Engineering and Technology-PET, Vol. 30, 2017, pp. 43-46.

[18] F. Kahoul, Elaboration et caractérisation de céramiques PZT dopé et détermination de la frontière morphotropique (FMP), Thèse de doctorat, Université Mohamed Khider-Biskra- Algérie, 2013.

[19] M.Azad, A.Avin, Scanning Electron Microscopy (SEM): A Review, Proceedings of the 2018 International Conference on Hydraulics and Pneumatics-HERVEX, Băile Govora, Romania, Vol. 2018, 2018, pp.77-85.

Chapter III

Structural and morphological study of the PCZT-FZS solid solution

III.1. Introduction

Current technology for manufacturing PZT-type ceramics with a perovskite structure tends to prepare compositions close to the morphotropic phase boundary (MPB).

The ferroelectric nature of $Pb(Zr_xTi_{1-x})O_3$ solid solution ceramics (PZT) and their derivatives was established in the 1950s. Subsequently, researchers have highlighted the intense piezoelectric activity of these materials, especially in compositions close to the morphotropic phase boundary (MPB), separating the tetragonal and rhombohedral phases.

Various methods are used to locate the compositions corresponding to the morphotropic phase boundary of PZT-type ceramics and its derivatives (addition of dopants), including **[1-3]**:

- X-ray diffraction analysis (**XRD**).
- Scanning electron microscopy (**SEM**).
- Phase analysis by infrared spectrometry (**IR**).

III.2. Ceramics synthesis and production

The main objective of this study is to locate the crystalline phase of the doped PZT solid solution. Our ceramic samples were synthesized using the ceramic method (the solid route), defined in detail in Chapter II. The chemical formula of our samples chosen for this study is:

$$\mathbf{Pb_{1-y}Ca_y[Zr_xTi_{0.98-x}(Fe_{1/5}Zn_{1/5}Sb_{3/5})_{0.02}]O_3}$$

Where: x = 0.49,0.50 and y=0.05, abbreviated in the text as PCZT-FZS, we will limit our experimental study to one series, varying:

- Zr content at site B of the PZT.
- The sintering temperatures (1100, 1150, 1200 and 1250°C).

(**Tab.III.1**) summarizes the different compositions that we are going to synthesize.

Table III.1: Different ceramic compositions

Sample number	Matrix	Composition PCZT-FZS (Zr/Ti)
1	$Pb_{0.95}Ca_{0.05}[Zr_{0.49}Ti_{0.49}(Fe_{1/5}Zn_{1/5}Sb_{3/5})_{0.02}]O_3$	PCZT-FZS (49/49)
2	$Pb_{0.95}Ca_{0.05}[Zr_{0.50}Ti_{0.48}(Fe_{1/5}Zn_{1/5}Sb_{3/5})_{0.02}]O_3$	PCZT-FZS (50/48)

III.3. Study of the stability criteria of the perovskite structure

(**Tab.III.2** and **III.3**) show the properties of each PZT component that we will use to check the stability conditions of the perovskite structure.

Table III.2: Ionic radii and percentage of elements in prepared matrices.

	Ionic radius (Å)	Valance number	Composition	
			No.1	**No.2**
Pb^{2+}	1.490	2	95	95
Ca^{2+}	1.000	2	05	05
Zr^{4+}	0.720	4	49	50
Ti^{4+}	0.605	4	49	48
Fe^{3+}	0.645	3	0.4	0.4
Zn^{2+}	0.740	2	0.4	0.4
Sb^{3+}	0.770	3	1.2	1.2
O^{2-}	1.400	2	100	100

Table III.3: Tolerance factor for different prepared ceramic compositions.

X	Samples	Geometric conditions (t)	Electroneutrality conditions
0.49	$Pb_{0.95}Ca_{0.05}[Zr_{0.49}Ti_{0.49}(Fe_{1/5}Zn_{1/5}Sb_{3/5})_{0.02}]O_3$	0.9815	+ 6.0000
0.50	$Pb_{0.95}Ca_{0.05}[Zr_{0.50}Ti_{0.48}(Fe_{1/5}Zn_{1/5}Sb_{3/5})_{0.02}]O_3$	0.9809	+ 6.0000

According to Goldschmidt, the perovskite structure is stable if: $0.75 < t < 1.06$ and this is verified for all the samples (see **Tab.III.3**). These compositions can therefore be synthesized as they all meet the stability conditions for a perovskite.

The 12g samples were prepared from the mixture of starting oxides according to the stoichiometry of the compositions:

Table III.4: Oxide mass requirements for the different compositions.

Oxides	mass (g)	
	Composition No.1	**Composition No.2**
PbO	7.9787	7.9679
$CaCO_3$	0.1872	0.1869
ZrO_2	2.2719	2.3152
TiO_2	1.4726	1.4406
Fe_2O_3	0.0119	0.0119
ZnO	0.0122	0.0122
Sb_2O_3	0.0654	0.0653

III.4. Morphological study of PCZT-FZS ceramics

In this section we discuss the results obtained from previous studies.

Density and porosity measurements are performed on 1.1g pellet samples of sintered PCZT-FZS powders.

The results of the theoretical density, experimental density, porosity, and densification rate of samples of the sintered PCZT-FZS system at different temperatures are reported in (**Tab. III.5**).

Table III.5: Experimental and theoretical density, densification rate and porosity for all samples.

T (°C)	Composition PCZT-FZS (Zr/Ti)	Mass (M)	Exp. density (g/cm^3)	Theo. density (g/cm^3)	Densification rate	Porosity (P)
1100	PCZT-FZS (49/49)	322.1302	**5.6425**	-	-	-
	PCZT-FZS (50/48)	322.5681	**4.9210**	-	-	-
1150	PCZT-FZS (49/49)	322.1302	**5.3611**	-	-	-
	PCZT-FZS (50/48)	322.5681	**5.2071**	-	-	-
1200	PCZT-FZS (49/49)	322.1302	**6.2194**	**8.0000**	**77.7424**	**0.2226**
	PCZT-FZS (50/48)	322.5681	**5.6451**	**8.0000**	**70.5633**	**0.2944**
1250	PCZT-FZS (49/49)	322.1302	**3.6565**	-	-	-
	PCZT-FZS (50/48)	322.5681	**5.2268**	-	-	-

III.4.1. Density

The study of density is necessary in order to optimize the sintering temperature. Material quality increases as density increases, and density increases as sintering temperature increases **[5]**.

Density measurements were carried out on pellet samples of diameter D = 13 mm and thickness e = 1.1 mm, and the density of PCZT-FZS was studied as a function of sintering temperature and Zr content. This study is necessary in order to optimize the sintering temperature and find the densest composition at the optimum sintering temperature, and to see the effect of the doping level on the density.

- **Changes in density as a function of sintering temperature**

The optimum sintering temperature is determined from the curves of density versus sintering temperature d = f (T). The maximum density corresponds to the product with the best electrical quality. (**Fig.III.1)** shows the density curves for all the PCZT-FZS samples as a function of sintering temperature.

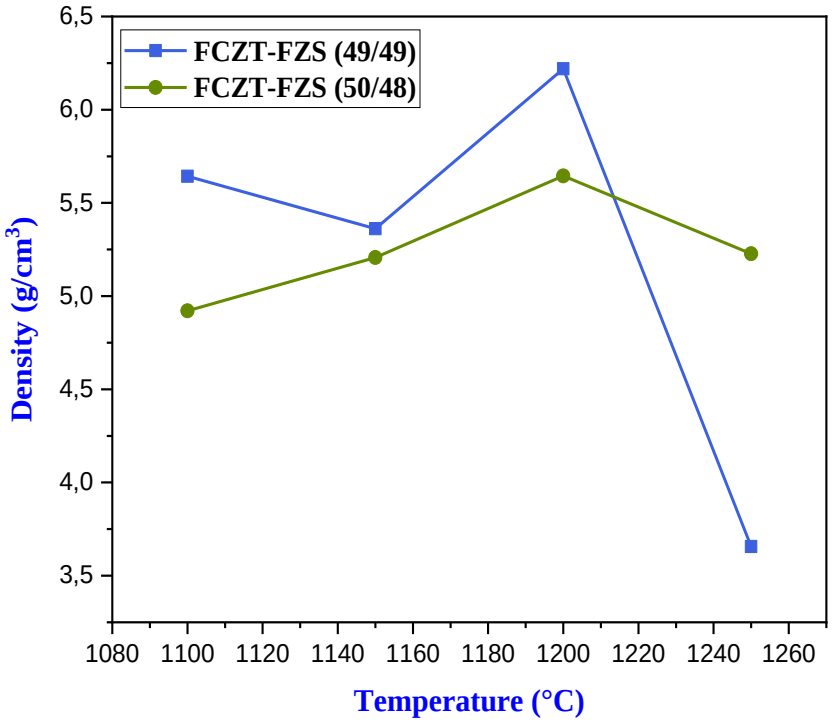

Figure III.1: Evolution of density as a function of sintering temperature.

The same pattern can be seen for all the curves: the density is minimal for a sintering temperature T_S = 1100°C, it starts to increase until it reaches a maximum value at a sintering temperature T_S = 1200°C, at which point the density starts to decrease again for samples sintered at a temperature T_S = 1250°C. We can therefore say that the sintering temperature **1200°C** is the optimum sintering temperature.

The increase in density implies a reduction in the number of pores, so the volume of the mesh decreases and, as a result, the structure becomes more compact.

The optimum sintering temperature depends on a number of factors, including the addition of impurities, the sintering rate, the holding time and the amount of $PbZrO_3$ added to minimize PbO volatilization.

- **Changes in density as a function of composition**

The evolution of the density of the different PCZT-FZS samples sintered at 1100, 1150, 1200 and 1250°C as a function of the Zirconium (Zr) content is illustrated in (**Fig.III.2**).

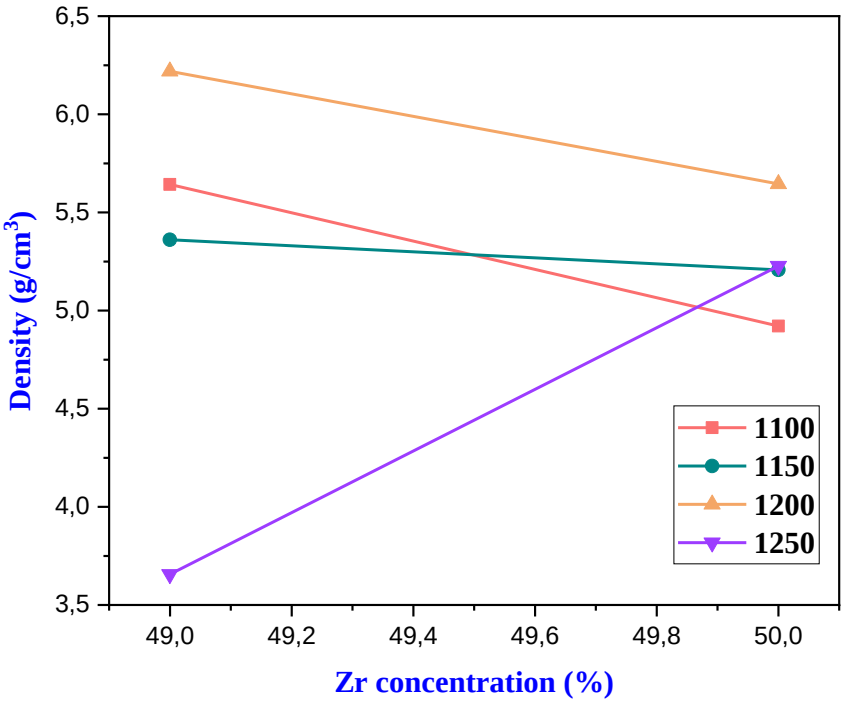

Figure III.2: Evolution of density as a function of Zirconium content.

(**Fig.III.2**) shows that the density increases for all the samples sintered at 1200°C with decreasing Zr content, reaching a maximum value of 6.2194 (g/cm^3) (77.74 % of the theoretical density) at Zr= 49% (sample no.1).

III.4.2. Porosity

(**Fig.III.3**) shows the variation in porosity as a function of sintering temperature for the different samples. We can see that the curves for porosity are the inverse of those for density, decreasing to a minimum corresponding to the maximum density at 1200°C, which confirms that the optimum sintering temperature is 1200°C.

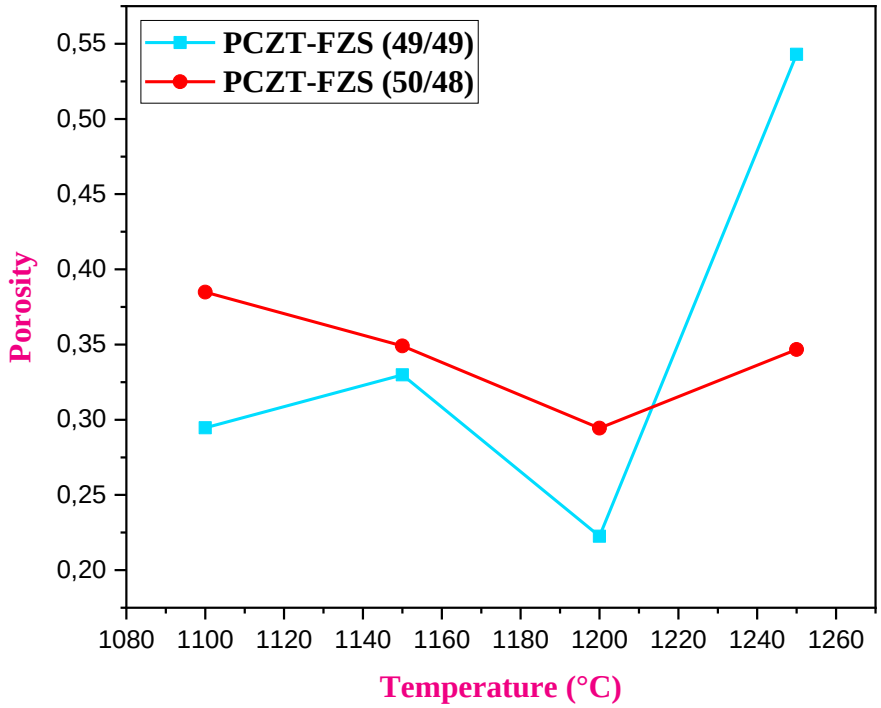

Figure III.3: Evolution of porosity as a function of sintering temperature.

(**Fig.III.4**) shows the evolution of the porosity of the various PCZT-FZS samples sintered at 1100, 1150, 1200 and 1250°C as a function of the concentration of Zirconium (Zr).

The minimum porosity value is for sample PCZT-FZS (49/49) (at 1200°C) is 0.222. This confirms that the density takes the maximum value for this sample.

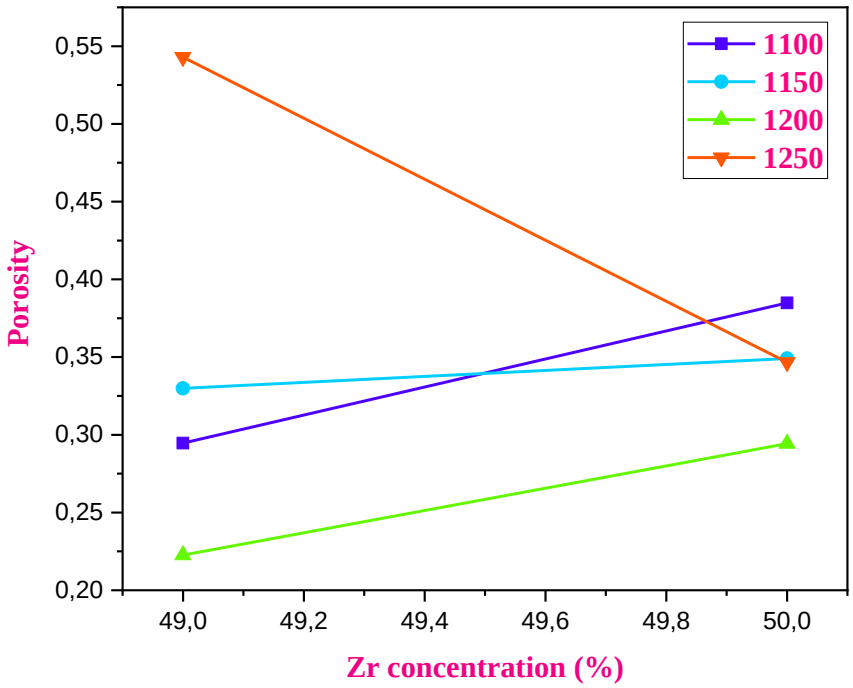

Figure III.4: Evolution of porosity as a function of Zirconium concentration (Zr%).

III.5. Microstructure

III.5.1. Structural study of PCZT-FZS

(**Fig.III.5**) shows typical XRD spectra of the rhombohedral phase (R) and the tetragonal phase (T). Below the curie temperature, the structure of PZT-type piezoelectric ceramics takes the form of two phases: one tetragonal (T) corresponding to the titanium-rich composition, the other rhombohedral (R) corresponding to the zirconium-rich composition. In the rhombohedral structure (R), the line (200) remains unchanged. In the tetragonal structure, the (200) line splits into two lines (200) and (002) **[1,6-8]**.

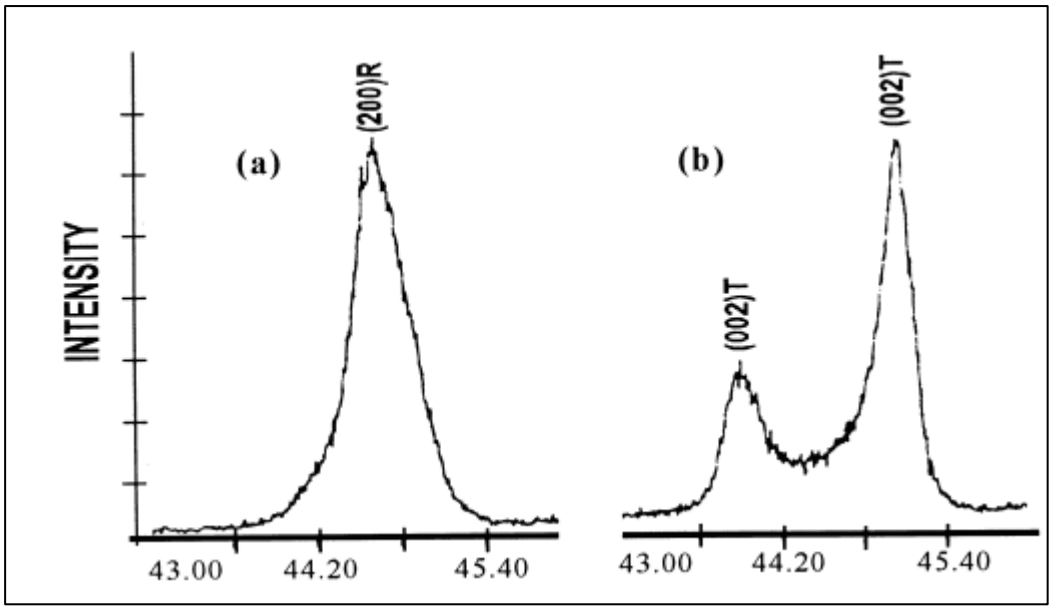

Figure III.5: Typical diffraction spectra of the Tetragonal (T) and Rhombohedral (R) phases.

The morphotropic phase boundary (T+R) is determined by observing the shapes of the diffracted lines. The appearance of the lines diffracted by samples where the two tetragonal and rhombohedral (T+R) phases coexist is represented by three types **[4,9]**.

- A pattern with three maxima (**Fig.III.6(a)**).
- Alignment with two maxima (**Fig.III.6(b)**).
- A curve with a maximum accompanied by an inflection point (**Fig.III.6(c)**).

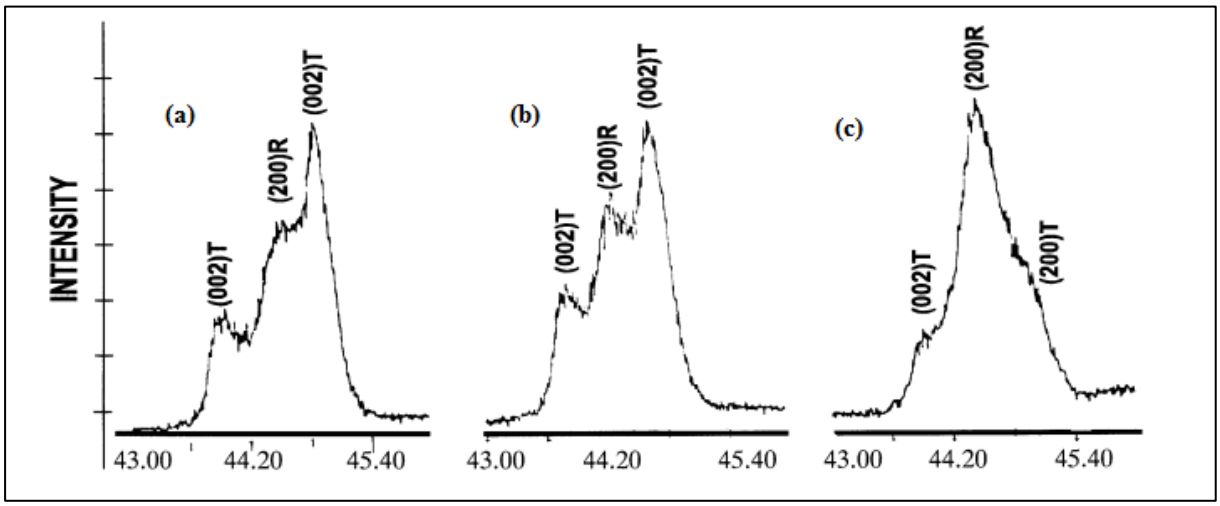

Figure III.6: The different shapes of the peaks characteristic of the coexistence of the (T+R) phase.

It should be noted that many researchers have reported that the coexistence of tetragonal (T) and rhombohedral (R) phases can be detected in several regions of the diffractogram spectrum. (**Tab.III.6**) below summarizes the most important regions in 2θ where the R and T phases coexist **[1]**.

Table III. 6: Region of coexistence of the Tetragonal-Rhombohedral phases and indexation of the corresponding planes.

2θ	**$(hkl)_T$**	**$(hkl)_R$**
21-23	(001) et (100)	(100)
30-33	(101) et (110)	(110) et (101)
37-40	(111)	(111) et (111)
43-47	(002) et (200)	(200)
53-56	(112) et (211)	(211), (211) et (211)

The sintered compounds $Pb_{0.95}Ca_{0.05}[Zr_xTi_{0.98-x}(Fe_{1/5}Zn_{1/5}Sb_{3/5})_{0.02}]O_3$ were carefully ground, then analyzed by X-ray diffraction to establish the crystallographic phases: tetragonal, rhombohedral and tetragonal-rhombohedral. The sintered samples were characterized using a D8 ADVANCE diffractometer (BRUKER) using copper K_α radiation (λ_{Cu} ($K_{\alpha1}$) =1.54 Å). The diffraction patterns

diffraction patterns are recorded in the angular range 10°< 2θ < 90° which appears to be sufficient for the identification of the different phases. X-ray diffraction on all PCZT-FZS samples is performed at room temperature.

The X-ray diffraction results for the two $CaCO_3$, ZnO, Fe_2O_3 and Sb_2O_3 doped PZT samples sintered at the optimum temperature of 1200°C are shown in (**Fig.III.7(a, b)**).

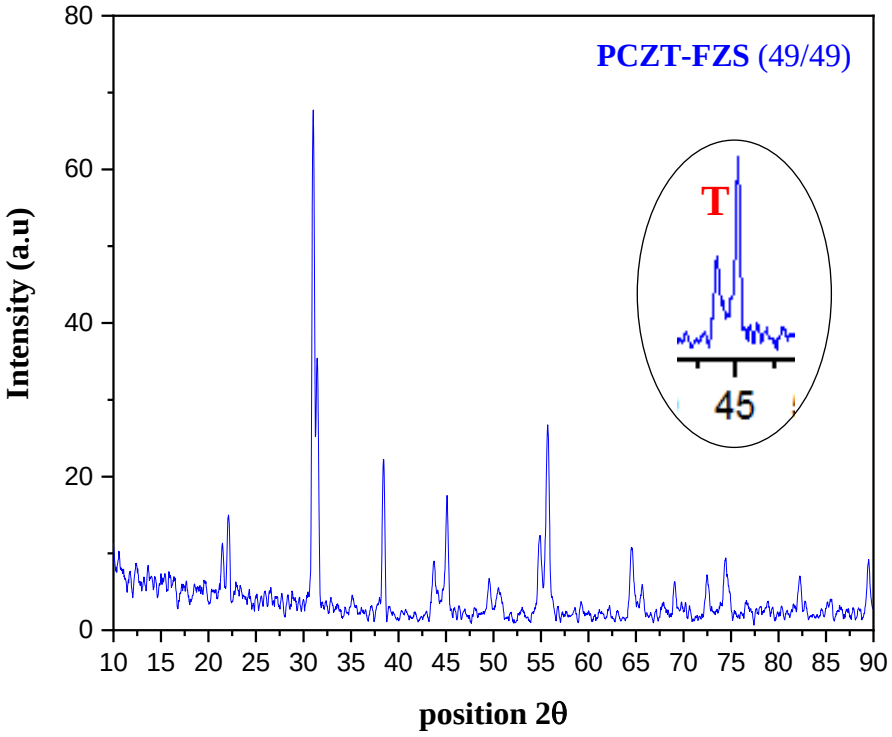

Figure III.7. a: X-ray diffraction (XRD) spectra of PCZT-FZS (49/49) sintered at 1200°C.

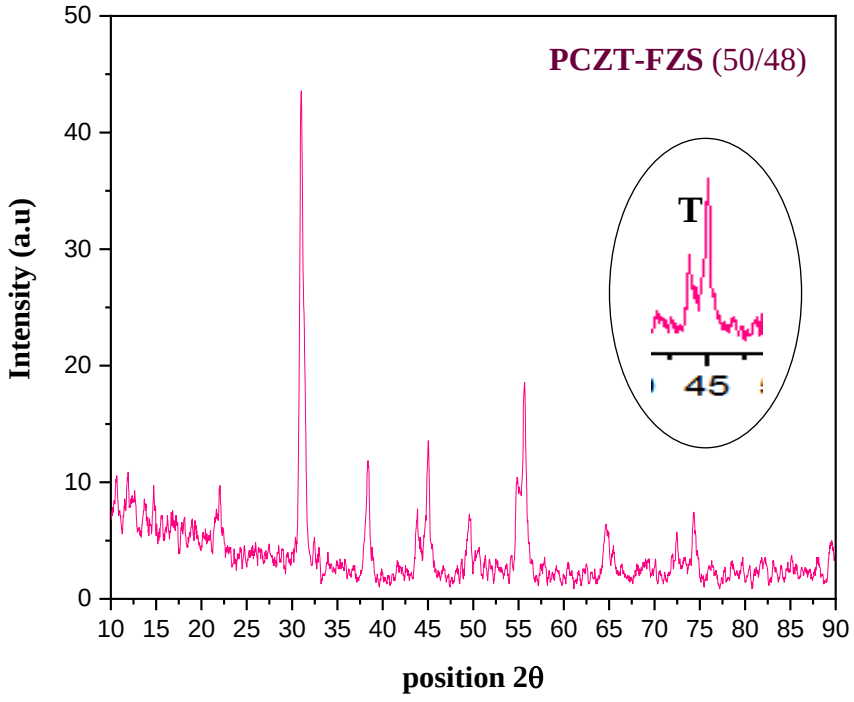

Figure III.7. b: X-ray diffraction (XRD) spectra of PCZT-FZS (50/48) sintered at 1200°C.

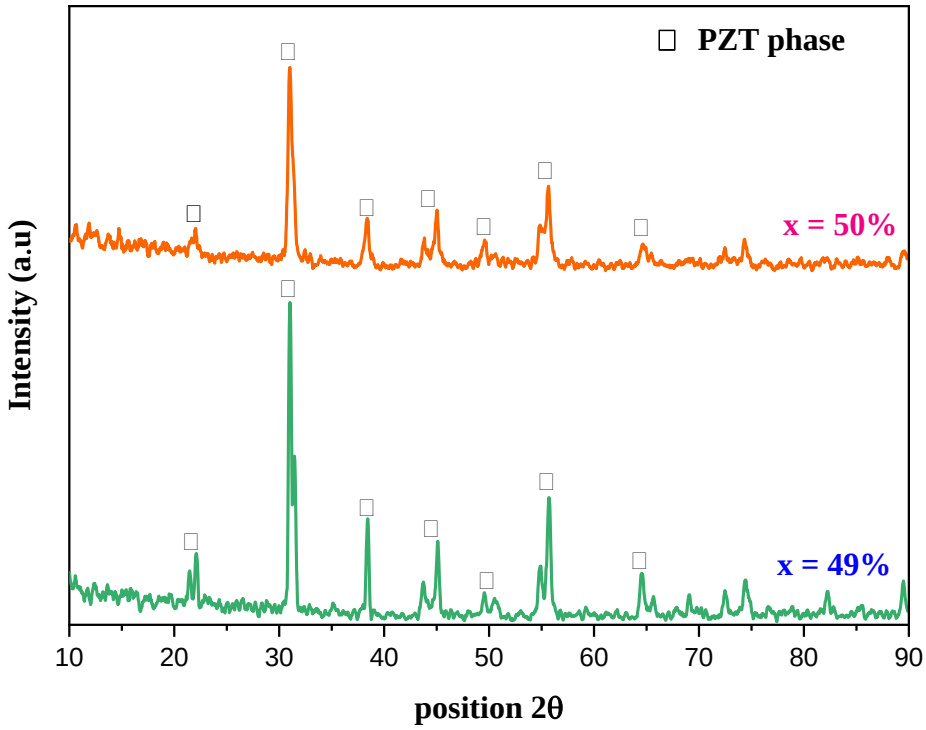

Figure III. 8: X-ray diffraction (XRD) spectra of PCZT-FZS ceramics sintered at 1200°C.

Table III.7: Nature of crystallographic phases at sintering temperature 1200 °C.

Zr concentration (%)	Nature of phases
49	T
50	T

From these results, it can be seen that there is a single tetragonal phase, characterised by peaks (002) and (200) in the 43-47° range. This phase is detected for all Zr = 49% and Zr =50% compositions sintered at 1200°C. We also note that there is no parasitic phase (pyrochlore) detected for all the samples.

We therefore conclude that the synthesised compositions are monophase materials.

The relative amount of pyrochlore phase is estimated using the following peak intensity ratio equation **[10]**:

$$\textbf{pyrochlore}\ (\%) = \frac{\mathbf{I_{pyro}}}{\mathbf{I_{pyro}} + \mathbf{I_{(110)}}} \times \mathbf{100} \ldots\ldots\ldots\ldots\ldots (\mathbf{III.1})$$

$\mathbf{I_{pyro}}$: The intensity of the pyrochlore peak.

$\mathbf{I_{(110)}}$: The intensity of the (110) peak.

- **Evolution of lattice parameters as a function of composition**

At a fixed temperature of 1200°C, we studied the evolution of the lattice parameters of the PCZT-FZS solution as a function of the Zr composition.

The lattice parameters are determined by the evolution of the position of the peak of the phase formed using Highscore Plus. (**Tab.III.8**) shows the crystalline parameters of our PZT sample after sintering at a temperature of 1200°C.

Table III.8: Calculated crystalline parameters of the prepared PZT sample.

Type of phase	Zr %	Mesh parameters					
		$a_T = b_T$ (Å)	c_T (Å)	α(°)	β(°)	γ(°)	(c_T/ a_T)
Tetragonal	49	4.0112	4.1344	90	90	90	1.0307
	50	4.0166	4.1374	90	90	90	1.0301

(**Fig.III.9**) shows the calculated crystalline parameters and distortion ratio as a function of zirconium content for all the ceramic samples sintered at the optimum temperature T_S = 1200°C.

It can be seen that these parameters are very sensitive to compositional variation, and the distortion of the c_T/a_T perovskite structure slightly decreases between [1.0301-1.0307] when the Zr concentration increases, the tetragonal phase (T) shows that the parameters a_T and c_T almost constant as the Zr concentration increases.

Generally speaking, there is a small difference between the values of the mesh parameters (a_T, and c_T) between compositions no. (1 and 2). Therefore, the smallness of this difference confirms that the perovskite structure is stable.

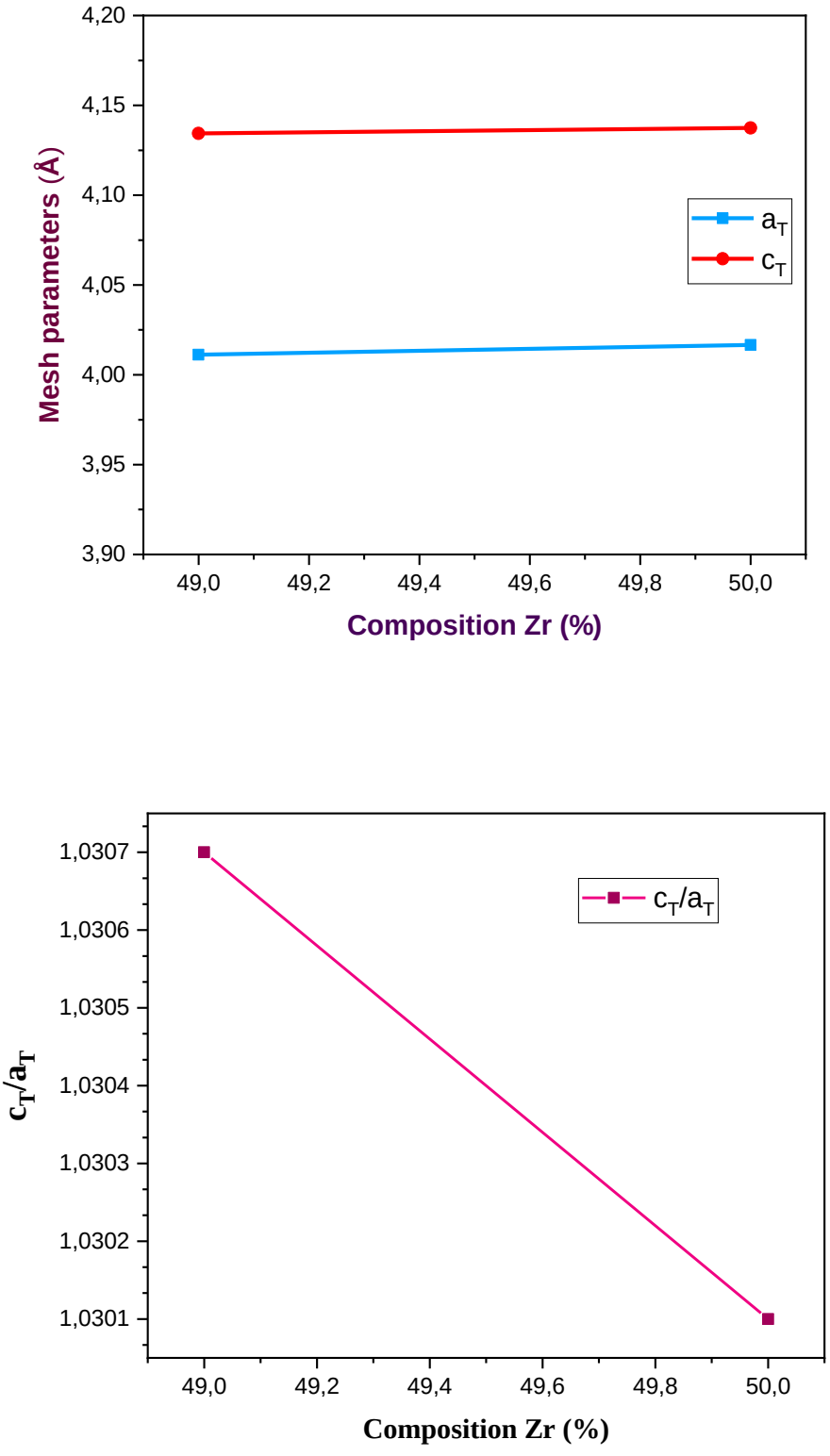

Figure III.9: Evolution of mesh parameters and distortion ratio as a function of Zirconium content for all samples sintered at 1200°C.

III.5.2. Scanning electron microscopy (SEM) characterization

Scanning electron microscopy provides information on the shape and size of the grains. This technique makes it possible to estimate the particle size distribution, the average grain size after sintering and qualitatively evaluate the presence of porosity and secondary phases.

(**Fig.III.10**), presents SEM micrographs for the composition $\mathbf{Pb_{0.95}Ca_{0.05}\ [Zr_xTi_{0.98-x}(Fe_{1/5}Zn_{1/5}Sb_{3/5})_{0.02}]O_3}$ at the optimum sintering temperature T=1200°C.

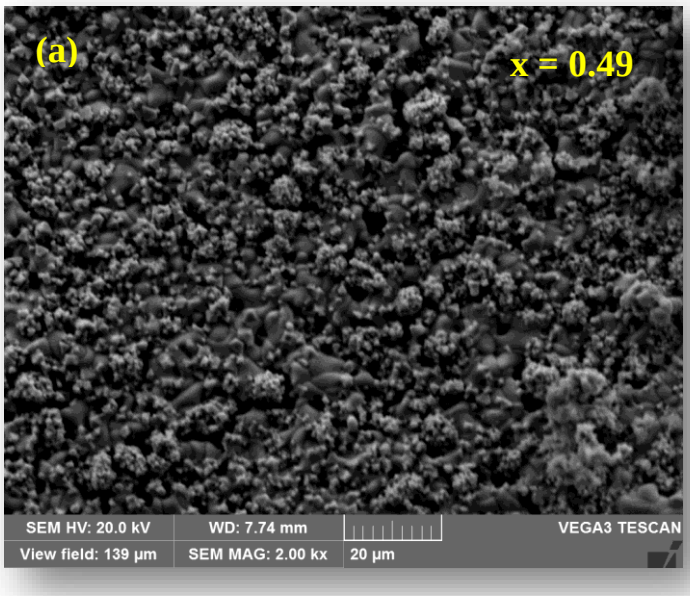

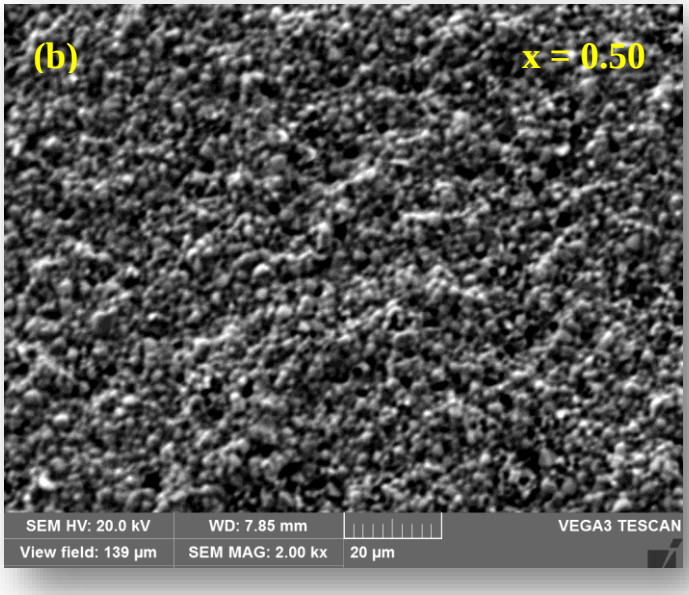

Figure III.10: SEM micrographs of the two compositions sintered at 1200°C: (a) - PCZT-FZS (49/49); (b) - PCZT-FZS (50/48).

The micrographs of the ceramics show that the materials are very dense (**Fig.III.10**), confirming the densification of the materials due to the diffusion mechanisms of the material during sintering. They also show low intergranular porosity for the compositions doped with 49 and 50% zirconium, and a narrow distribution of grains in each sample, as well as the appearance of some unreacted starting materials, which may be due to the insufficient sintering temperature…etc.

It can be seen that the average grain size calculated by "visiomètre" software for the first (**x = 0.49**) and second (**x = 0.50**) samples is **3.21 µm** and **2.19 µm** respectively, and the grain distribution is uniform throughout. It is clear that porosities are not completely eliminated during sintering for both compositions, which could influence the electrical and electromechanical properties of these perovskite materials, which are highly dependent on their microstructures.

Micrographs of PCZT-FZS compositions sintered at 1200°C show the absence of the secondary phase (the pyrochlore phase), which can be identified by their pyramidal shape **[1]**.

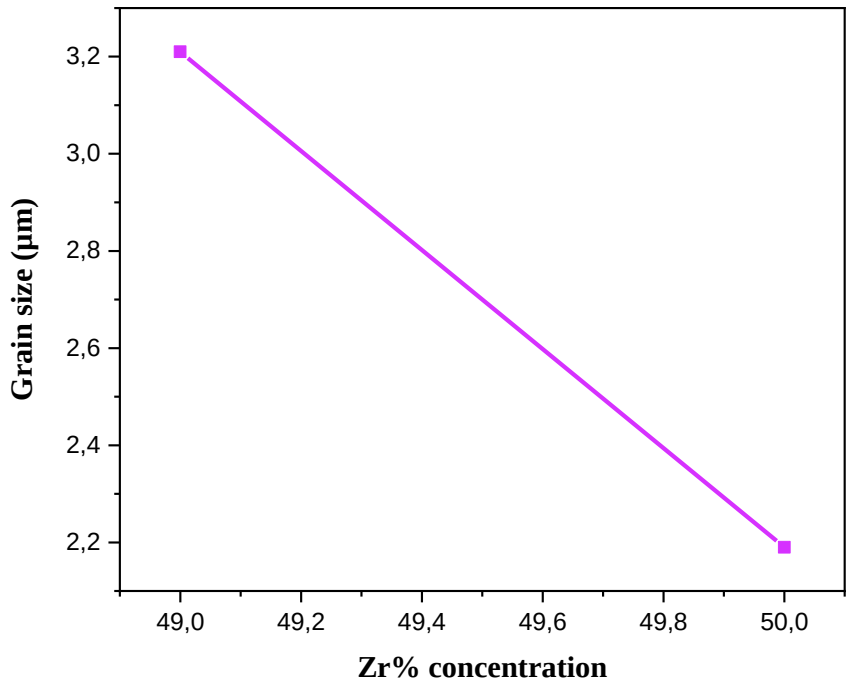

Figure III.11: The evolution of average grain size as a function of zirconium content for all PCZT-FZS compositions sintered at 1200°C.

(**Fig.III.11**) shows the evolution of the average grain size as a function of the zirconium content. It can be seen that the average grain size decreases with increasing Zr.

III.5.3. Phase analysis by infrared spectrometry (IR)

The use of Fourier Transform Infrared (FTIR) spectroscopy is only a complementary step that provides further information on the formation temperature of the PZT solid solutions.

Analysis of the powder treated at ambient temperature, at calcination temperature 800°C and at optimum sintering temperature 1200°C by IR (**Fig.III.12** (**a** and **b**)).

For powders calcined at 800°C and sintered at 1200°C, we observed the presence of an intense band at around 600 cm^{-1} attributed to the vibration of the O-B-O bond, confirming the formation of the perovskite (ABO_3) phase of PZT.

For powders at ambient temperature, an intense band at around 1400 cm^{-1} was observed, corresponding to the vibration of the B-O bond.

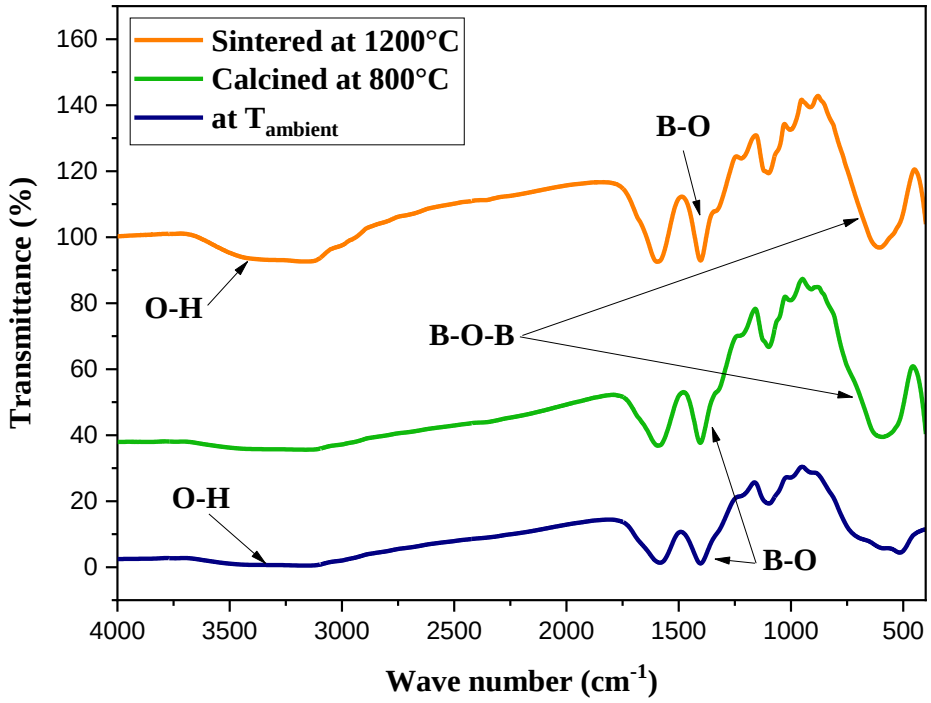

Figure III.12.a: IR absorption spectrum of the PCZT-FZS (49/49) composition at ambient, 800°C calcination and 1200°C optimum sintering temperatures.

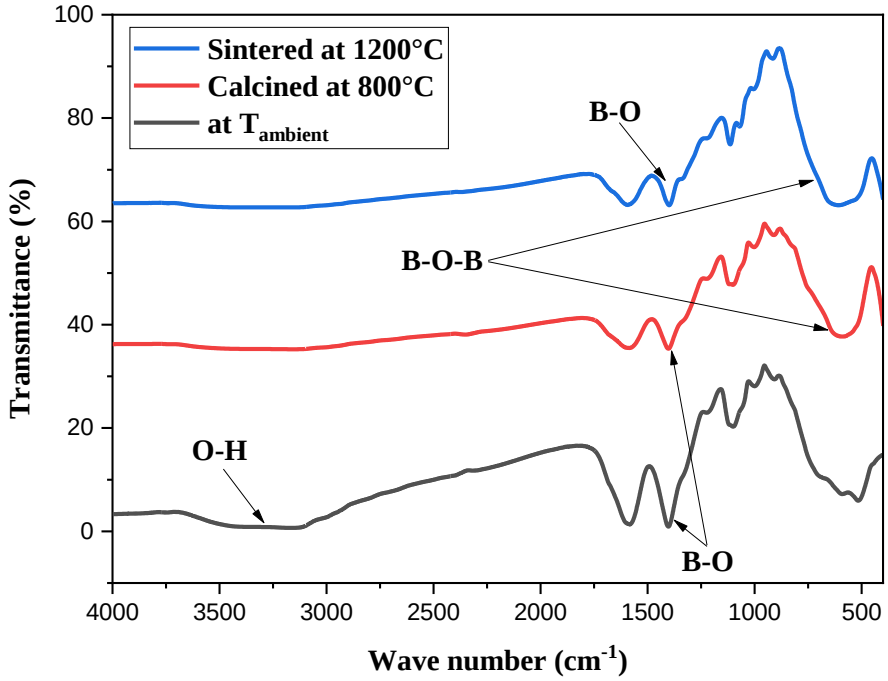

Figure III.12.b: IR absorption spectrum of the PCZT-FZS (50/48) composition at ambient, 800°C calcination and 1200°C optimum sintering temperatures.

We also observe the appearance of a band at around 1600 cm^{-1} that may be caused by some unreacted starting material, which is consistent with the results obtained by SEM, and the OH band for water, which is mostly due to atmospheric humidity.

Bibliographic References

[1] K. Megherbi, S.Ferhat , Influence de la température de frittage sur les propriétés structurales et physiques dans le système ternaire PLZT-FZS, Mémoire de Master, Université Mohamed Khider-Biskra-Algérie, 2019.

[2] M.Abba, Synthèse, caractérisation et étude Des propriétés Piézo-électriques des céramiques de type PZT : $Pb_{1-y}\ La_y\ [Zr_x\ Ti_z\ (Mo_{1/3}\ In_{2/3})_{1-(x+z)}]_{\ 1-y/4}\ O_3$, Thèse de doctorat, Université Mohamed Khider-Biskra-Algérie, 2013.

[3] A.Meklid **,** Elaboration, caractérisation et étude des propriétés diélectriques et électromécaniques d'un nouveau matériau de céramique de type Zirconate-Titanate de plomb (PZT)**,** Thèse de doctorat, Université Mohamed Khider-Biskra-Algérie,2018.

[4] R.K.Abdelli, Synthèse et caractérisation d'un matériau de la structure pérovskites à base plomb, Mémoire de Master, Université Mohamed Khider-Biskra- Algérie ,2018.

[5] F.Kahoul, L.Hamzioui et A.Boutarfaia ,Synthèse et caractérisation de nouvelles céramiques PZT-SFN, International Days of Organometallic Chemistry and Catalysis JICOC, 2012, pp. 58-67

[6] A.I. Kingon, P.J. Terblanché, J.B. Clark, Effect of Reactant Dispersion on Formation of PZT Solid Solutions, Ceramics International, Vol. 8, No.3, 1982, pp. 108-114.

[7] A. K. Zak, W.H. A. Majid, Effect of Solvent on Structure and Optical Properties of PZT Nanoparticles Prepared by Sol-gel Method, in Infrared Region, Ceramics International, Vol. 37, No.3, 2011, pp.753-758.

[8] A.Boutarfaia, Investigati ons of co-exist ence region in lead zirconate-titanate solid solutions: X-ray diffraction studies, Ceramics International ,Vol.26, No.6, 2000, pp.583-587.

[9] A.Boutarfaia, Study of the solid state reaction and the morphotropic phase boundary in $Pb(Zr,Ti)O_3$-$Pb(Fe_{1/5},\ Ni_{1/5},\ Sb_{3/5})O_3$ ceramics , Ceramics International ,Vol.27, No.1, 2001, pp.91-97.

[10] H. Menadra, Z. Necira , K. Bounabe, M. Abba , A. Meklid, A.Boutarfaia, Structural and electrical characterization of La^{3+} substituted PMS-PZT (Zr/Ti:60/40) ceramics, Materials Science-Poland, Vol. 36, No.1, 2018, pp. 1-6.

General Conclusion

General Conclusion

The work carried out during this dissertation is part of the study of PZT-type piezoelectric ceramics with a perovskite structure Pb (Zr_x Ti_{1-x}) O_3. This study is conducted by varying x and performing substitutions at the A and B sites of the perovskite structure with a mixture of acceptor and donor dopants ($CaCO_3$, Fe_2O_3, ZnO, Sb_2O_3), with the aim of synthesizing new materials.

This study addresses two main parts: the first part concerns the synthesis of PCZT-FZS from a mixture of oxides using a conventional process. The second part is devoted to the morphological and structural study of a ternary system with the general formula:

$$\mathbf{Pb_{1-y}Ca_y[Zr_xTi_{0.98-x}(Fe_{1/5}Zn_{1/5}Sb_{3/5})_{0.02}]O_3}$$ with **y = 0.05** and **x = 0.49, 0.50**.

To achieve our objective, the elaboration step followed for the synthesis of our ceramic is the solid-state method, known as the "classic method," which is the most used in laboratories and industry due to its simplicity and low cost.

Thermal treatment at different sintering temperatures of 1100°C, 1150°C, 1200°C, and 1250°C is applied to these samples in order to homogenize the solid solution and stabilize the crystallographic structure.

Three analyses are used for morphological and structural identification: X-ray diffraction (XRD), scanning electron microscopy (SEM), and infrared spectroscopy (IR).

The various analysis methods utilized have allowed us to draw the following conclusions:

- The effect of sintering temperature on density and porosity was studied to determine the optimal sintering temperature. This temperature (1200°C) corresponds to the maximum density value and thus the minimum porosity value, which also corresponds to the product with the best properties.
- The X-ray diffraction study confirmed the existence of the PZT perovskite phase. The diffractograms of the different samples sintered at 1200°C show that the PZT phase has a tetragonal structure. The lattice parameters of T phase (a_T, c_T) are sensitive to zirconium content.

- The grain distribution is almost uniform across the entire surface of the sample. The average grain size decreases with the increase in Zr content, with a minimum value observed for sample no.2 (x = 50%) (2.19 µm) and a maximum value (3.21 µm) for sample no.1 (x = 49%). The micrographs of PCZT-FZS compositions sintered at 1200°C showed the absence of the secondary phase (pyrochlore phase), which is identifiable by its pyramidal shape. This observation is confirmed by XRD.
- The IR analysis for powders at ambient temperature, calcined at 800°C and sintered at 1200°C showed the presence of a band between 850 cm^{-1} and 450 cm^{-1}, which is attributed to the vibration bands of the O-B-O bond. This characterizes the absorption band of the perovskite structure.
- Composition no.1 (49/49) is the best compared to the other sample because of its higher density, lower porosity and larger average grain size.

Based on the results obtained, it can be said that the PCZT-FZS ceramics have a good densification, as confirmed by XRD, IR and SEM analyses. However, it is considered to be average compared to the results of previous studies. This suggests that their piezoelectric and dielectric properties should be studied to determine their suitability for industrial applications.

République Algérienne Démocratique et Populnire
inistère de l'Enseignement Supérieur et de la Recherche Scientifique
Université Med Khider Biskra
aculté des Sciences Exactes et des Sciences de la Nature et de la Vie
Département des Sciences de la Matière
Filière de Chimie

الجمهورية الجزائرية الديموقراطية الشعبية
وزارة التعليم العالي و البحث العلمي
جامعة محمد خيضر بسكرة
كلية العلوم الدقيقة و علوم الطبيعة و الحياة
قسم علوم المادة
شعبة الكيمياء

تصريـــح شرفـــي

خاص بالالتزام بقواعد النزاهة العلمية لإنجاز بحث

(ملحق القرار 1082 المؤرخ في 2021/12/27)

أنا الممضي أسفله،

السيد(ة):.....حاسمي..فدوى..أريج.....

الصفة: طالب سنة ثانية ماستر كيمياء تخصص:..كيمياء..المواد..

الحامل(ة) لبطاقة التعريف الوطنية رقم:.....199901888..... الصادرة بتاريخ:..2024..01..02..

المسجل بكلية: العلوم الدقيقة وعلوم الطبيعة والحياة قسم:..علوم..المادة.....

والمكلف بانجاز أعمال بحث : مذكرة ماستر في الكيمياء

عنوانها: .....Effect of doping and sintering temperature on the structural properties of a dielectric ceramic.....

أصرح بشرفي أني ألتزم بمراعاة المعايير العلمية والمنهجية ومعايير الأخلاقيات المهنية والنزاهة الأكاديمية المطلوبة في انجاز البحث المذكور أعلاه وفق ما ينص عليه القرار رقم 1082 المؤرخ في 2021/12/27المحدد للقواعد المتعلقة بالوقاية من السرقة العلمية ومكافحتها.

التاريخ: .....2024-05-30.....

إمضاء المعني بالأمر

Hachemi